Abstract

As the climate continues to change, humanity is increasingly under threat of the associated environmental consequences. Sustainable cities, resilient in the face of changing climate, are needed as a habitat for humanity. Cities are complex and there are many factors that influence their resiliency and health. Some recent efforts have focused on increasing urban green spaces and their associated ecosystem services as a way to address multiple urban issues synergistically. One green infrastructure technology, green roofs, provide the opportunity to add green spaces to cities without losing valuable real estate at street level, while providing multiple ecosystem services not provided by a traditional roof. Despite increasing construction of green roofs within urban centers, the performance of green roofs has not been adequately measured quantitatively.

My work aims to enhance our understanding of the thermal and hydrologic performance of a large extensive green roof. Further, to bridge the gap between research and the practice of engineering, this study also considers the performance of commonly applied models in predicting green roof performance. Empirical data are collected at Syracuse, New York's OnCenter green roof over the course of eight years, including rainfall, runoff, soil moisture, thermal roof properties, and meteorological parameters.

As we collectively work to adapt to a changing climate and to design more resilient cities, green roofs are being investigated for their role in the overall energy balance of buildings. In the first part of this work, I determine the thermal properties of the OnCenter green roof using temperature sensors installed during roof construction. Temperature sensors were installed at five stations across the roof to measure temperature at four depths within the roof layers. Heat fluxes range from -5.76 W m^{-2} to 9.46 W m^{-2}. Negative (downward) heat flux is found during summer

and early fall, and positive (upward) heat flux dominates during the heating season. Solar radiation can heat the upper layers of the roof significantly above ambient air temperatures during the summer. Accumulated snow acts as an insulator during the winter months. Thermal resistance, R, is determined during a two-week period with significant snow accumulation, during which time heat flow through the roof reached a quasi-steady state. Thermal resistance for the overall roof is found to average 3.1 m^2 K W^{-1}. The largest individual thermal resistance is from the extruded polystyrene insulation layer (R = 2.6 m^2 K W^{-1}). Overall, the green roof dampens the temperature or heat flux responses often observed on urban roofs. Vegetation and substrate layers may be used in addition to insulation but are not recommended in lieu of insulation for a Central New York climate.

Success in creating resilient cities also relies on the ability of urban areas to function with the hydrologic changes brought on by climate change. Green roof hydrologic performance reported in the literature varies widely – the result of differences in green roof design and climate, as well as limitations to study design and duration. In the second part of this work, I quantify the hydrologic performance of the extensive green roof on the OnCenter over a period of 21 months. Over the monitoring period, the roof retains 56% of the 1062 mm of rainfall recorded. Peak runoff is reduced by an average of 65%. Eleven events exceed 20 mm and are responsible for 38% of the rainfall and 24% of the annual retention. Retention in the summer is lower than that in the fall or spring, as a result of greater rainfall intensity during the period sampled. Soil moisture during winter months remains high, reducing the ability of the roof to retain rainfall volume from new events. Comparison of seasonal data demonstrates the strong influence of rainfall intensity on runoff and the effect of initial soil moisture on event retention.

Green roofs are being applied as a modern stormwater management tool at an increasing rate across the globe. To apply this technology, however, practitioners must conform with regulatory requirements, for which two methods dominate: the SCS Curve Number method and the Rational method. Universally accepted model inputs (CN and C_v respectively) do not exist for green roofs, and likely vary based on roof composition and region. In this study, I calibrate CN and Cv using nearly seven years of rainfall-runoff data from the OnCenter green roof. Median event CN and a least-squares estimate both result in a CN of 96. When season is included in the analysis, calculated CN in the winter (CN = 99) exceeds that generally used to model an impervious surface (CN = 98), while the summer has the lowest CN (95). Event C_v ranges from 0 to 0.99 with a median of 0.06, however C_v increases with depth of rainfall. Overall, the values skew towards the higher side of what is reported in the literature and closer to impervious surfaces than natural vegetated surfaces. This pattern may indicate the inappropriateness of the currently accepted methods to fully capture the performance of green roofs and their contribution to urban stormwater management. The results of this study suggest overestimating the hydrologic performance of a green roof via lower or inaccurate curve numbers may have negative consequences in practice.

This research makes a valuable contribution to our understanding of green roofs and their performance within the context of the Central New York climate. The contribution of this work, however, extends beyond the region by highlighting future areas of research and capturing the inability of commonly-used hydrologic models to accurately account for the performance of green roofs. The results of this work inform the design and adoption of green roofs by practitioners, and the regulations enacted by policymakers that influence our built environment.

THERMAL AND HYDROLOGIC PERFORMANCE OF AN EXTENSIVE GREEN ROOF IN SYRACUSE, NEW YORK

by
Mallory Squier-Babcock

B.S., Pennsylvania State University, 2009
M.S., Carnegie Mellon University, 2010

DISSERTATION
Submitted in partial fulfillment of the requirements for the degree of
Doctor of Philosophy in Civil Engineering

Syracuse University
June 2023

Acknowledgements

I would like to express my gratitude to my advisor, Dr. Cliff Davidson, for his support throughout my doctoral studies. His consistent encouragement and challenge guided me both in this work and in the development of skills that will serve me my whole life.

I would like to thank my committee members Dr. Charles Driscoll, Dr. Elizabeth Carter, and Dr. Andria Costello Staniec for their support in the completion of this work. I would also like to thank Dr. Jensen Zhang for agreeing to chair my committee.

This work would not have been possible without Han Pham and the Onondaga County Facilities Management Department. I would like to thank them for their assistance and permission to work at the OnCenter, especially Billy Brazell, Charles Campbell, Joseph Clemens, Chris Denny, Lenny Graf, Frank Santorelli, and Archie Wixson. Many students assisted in the installation of the instrumentation on the roof, in testing equipment in the lab, and maintaining the roof equipment over the years. I would like to thank all of them, but especially Dr. Pavle Bujanovic, Rich Murray, Joey DiStefano, J.B. Ahmad, Tenzin Lama, Chris Weiman, Katie Duggan, Joshua Saxton, Zhi Cui, Zhuyu Dai, and Xin Chen.

The valuable experience I gained as a practicing engineer at EDR, DPC in Syracuse, New York motivated the final chapter of this work. I would like to thank my colleagues there for teaching me about the practice of engineering, especially Justin Chiera, P.E., Carolyne Bean, P.E., and Tom Dussing, P.E. I would also like to thank Mary Steblein, P.E., my current colleague for reviewing the manuscript of the final chapter and providing her valuable perspective as a stormwater expert and Town Engineer.

To the many friends I made through the years in Syracuse, thank you for these experiences. In particular, Will, Heather, Emily, and Mike, I will cherish the memories we made and hope to make many more together. To Dr. Carli Flynn, what a journey, thank you for your years of support and friendship. I'm grateful I shared this journey with you.

I would like to express my love and thanks to my incredible husband, Tom Babcock, for his encouragement and support over the years. I thank my sister, Erin Squier, for always speaking the truth and reminding me to move forward. And to my parents, who always encouraged me to value and pursue knowledge throughout my life, I cannot express the level of gratitude I have for the gift you gave me. Finally, to my sons Gideon and Callum, who came into my life in the last stage of this journey and reminded me how strong I am, I dedicate this work to you. May you enthusiastically pursue new knowledge every day of your lives.

Chapter 1. Introduction 1
1.1 Thesis Overview 1
1.2 Background 1
1.2.1 Thermal Performance of Green Roofs 3
1.2.2 Hydrologic Performance 5
1.2.3 Stormwater Models 9
1.3 Aims and Objectives 10
1.4 Limitations 10
1.5 Structure 11

Chapter 2. Study site and Instrumentation 12
2.1 Study site 12
2.2 Instrumentation 16
2.2.1 Temperature 18
2.2.2 Soil moisture and sensor calibration 18
2.2.3 Runoff and magmeter calibration 21
2.2.4 Rainfall and weather 24

Chapter 3. Heat flux and seasonal thermal performance of an extensive green roof 26
3.1 Introduction 26
3.2 Methods 27
3.3 Results & Discussion 28
3.3.1 Heat flux and thermal resistance 28
3.3.2 Annual trends 29
3.3.3 Summer thermal behavior 31
3.3.4 Winter thermal behavior 33
3.4 Conclusion 35

Chapter 4. Hydrologic performance of an extensive green roof in Syracuse, NY 37
4.1 Introduction 37
4.2 Methods 38
4.3 Data analysis 38
4.3.1 Event analysis 38
4.3.2 Event plot statistical analysis 40
4.3.3 Evapotranspiration analysis 40

4.3.4 Weather during the study period 41
4.4 Results and Discussion 44
4.4.1 Green roof performance 44
4.4.1.1 Performance by event size 48
4.4.1.2 Performance by season 49
4.4.1.3 Evapotranspiration 50
4.5 Conclusions 56

Chapter 5. Green roofs in our cities: An analysis of two commonly-used modeling methods for the application of green roof technology 58
5.1 Introduction 58
5.2 Methods 59
5.2.1 Curve Number 59
5.2.1.1 Curve Number step function 60
5.2.1.2 The initial abstraction term 61
5.2.2 Rational Method 61
5.3 Results & Discussion 63
5.3.1 Data set 63
5.3.2 Curve number 64
5.3.2.1 Curve number determined from events 64
5.3.2.2 Evaluate curve number using step number function 69
5.3.2.3 Calibrate curve number with changing lambda 70
5.3.2.4 Performance of other CN values 70
5.3.2.5 Seasonal comparison of CN estimate 71
5.3.3 Rational Method 72
5.3.3.1 Determine Cv from rainfall-runoff pairs 72
5.3.3.2 Regional exponential model for Cv 74
5.3.4 OnCenter green roof and local regulations 76
5.4 Conclusions 78

Chapter 6. Conclusions 80
6.1 Summary 80
6.2 Thermal Findings 80
6.3 Hydrologic Findings 81
6.4 Modeling Findings 82

6.5 Contributions 83
6.6 Limitations and Future Work 84
Appendix A 86
Appendix B 88
References 91
VITA 99

List of Figures

Figure 2.1 Looking south on the OnCenter green roof during the Summer 2013 13
Figure 2.2 Location of roof drains and drain conduits on the OnCenter green roof..... 15
Figure 2.3 Roof layers and temperature sensor locations within the OnCenter green roof..... 15
Figure 2.4 Location of temperature profiles and equipment on the OnCenter green roof..... 17
Figure 2.5 Water Content Reflectometer and constructed PVC box with substrate during calibration 20
Figure 2.6 Volumetric water content and period for multiple trials during soil moisture sensor calibration. 21
Figure 2.7 Magmeter pipe configuration prior to initial install 22
Figure 2.8 Calibration curve developed from field calibration of an electromagnetic flowmeter using a nutating disc meter and a water source..... 24
Figure 3.1 Temperature in layer G at stations 1 and 5 during Winter 2015. 28
Figure 3.2 Heat flux across the insulation layer from September 2014 – September 2015..... 30
Figure 3.3 Average temperature at each layer for all 5 stations during Summer 2015 31
Figure 3.4 Insolation during 11 days in June and July 2015. 33
Figure 3.5 Average temperature at each layer during 19 days of Winter 34
Figure 4.1 Conceptual diagram of rainfall and runoff 39
Figure 4.2 Historic temperatures as recorded from 1950-2010 and actual temperatures from October 2014 to July 2016..... 41
Figure 4.3 Tukey box and whiskers plots for the monthly historical precipitation from 1950-2010 as recorded at the Syracuse Hancock International Airport..... 42
Figure 4.4 Rainfall duration and depth with recurrence intervals in years for Syracuse, New York 43
Figure 4.5 Runoff and retention from the OnCenter green roof, designed to hold a 25.4 mm rainfall event, grouped by event size 47
Figure 4.6 Event exceedance probability for runoff depth separated by season for the OnCenter green roof..... 50
Figure 4.7 Average and daily evapotranspiration as quantified on the OnCenter green roof between April 25, 2015 and July 8, 2016 52
Figure 4.8 Seasonal trends in average daily evapotranspiration relative to maximum daily insolation on the OnCenter green roof..... 54
Figure 4.9 Average daily evapotranspiration relative to daily initial soil moisture on the OnCenter green roof. 54
Figure 5.1 Runoff and retention from the OnCenter green roof, designed to hold a 25.4 mm rainfall event grouped by event size 63
Figure 5.2 Event curve number in relation to rainfall and runoff depth 65
Figure 5.3 Observed rainfall-runoff pairs and modeled runoff for four curve numbers..... 68
Figure 5.4 One large rain event (Total depth = 71.8 mm) on the OnCenter green roof..... 73
Figure 5.5 Comparison of estimated volumetric runoff coefficients and three exponential models fit for different climate zones..... 75
Figure A.1 Temperature for 5 layers of the OnCenter green roof measured in June 2015.....95
Figure A.2 Temperature for 5 layers of the OnCenter green roof measured in January 2015 96
Figure B.1 313 observed rainfall-runoff pairs (rainfall depth > 2 mm) are compared with modeled runoff using four curve numbers.....97

List of Tables

Table 2.1. Average climatic conditions by season in Syracuse, NY 12
Table 2.2 Thickness and manufacturer R-value of material layers 16
Table 2.3 Variables measured, sensors, and accuracy range for OnCenter green roof monitoring system. 17
Table 3.1 Calculated R-values at four stations 28
Table 4.1 Detention metrics for 39 events where runoff occurred, and data is collected at the 5-minute timestep. 44
Table 4.2 Details for 11 events which exceed 20 mm in total depth 48
Table 4.3 Retention by season for the OnCenter green roof. 49
Table 5.1 Goodness of fit criteria NSE and R^2 for model assessment of four curve numbers. ... 67
Table 5.2 Efficiency criteria for two curve numbers and lambda = 0.05 69
Table B.1 Details for 35 events which exceed 20 mm in total depth. 98

Chapter 1. Introduction

1.1 Thesis Overview

The restoration of natural processes to the urban environment through green infrastructure helps mitigate urban hydrologic issues created by the modern built environment. Green infrastructure can also contribute to an urban area's climate resilience. Despite increasing adoption of all green infrastructure technologies, gaps remain in our understanding of their performance. Unlike gray infrastructure, green infrastructure takes advantage of the natural environment and therefore a one-size-fits-all solution does not exist. In this dissertation I aim to fill some of these gaps on one prominent green infrastructure project in the northeastern U.S. climate of Syracuse, NY. In this chapter, we first provide a background and context in which to set this work, followed by details of the research problem, the aims of this research, and significance and limitations of the work.

1.2 Background

More than 50% of the world's population today lives in cities, and this is expected to reach 66% by 2050 (United Nations 2014). The increase in growth has resulted in an expanding number of cities that are faced with multiple environmental threats including urban heat islands, air and water pollution, urban flooding, and excessive noise. Research has begun to consider the problems facing urban centers and to develop methods to increase the sustainability, resilience, and quality of life in cities (Manning 2011). Multi-faceted approaches that implement decentralized solutions, unique to local needs, are favored as existing infrastructure and limited finances restrict the application of traditional methods. Green infrastructure (GI) is one category of solutions which attempts to integrate quasi-natural surfaces with the existing built

environment. GI technologies provide a variety of services, and their performance can be optimized for the regional climate.

One noteworthy example of GI is the green roof, where a variety of vegetation can be grown in engineered soil. Early evidence of green roofs in recorded history includes their implementation on institutional buildings in ancient Rome, where they were reportedly constructed in response to increasing urbanization. Early Nordic cultures integrated turf and seaweed into their roofing structure to insulate and provide protection from the elements. Hanging or vertical gardens have been found in many cultures throughout history including India, Russia and France, and pre-Columbian Mexico (Peck et al. 1999). The modern green roof industry has its roots in turn of the 20th century Germany, where vegetation was employed to reduce solar radiation damage to roof structures and act as a fire-retardant (Köhler et al. 2003). New York City's Rockefeller Center, constructed in 1931, has one of the first modern green roofs in the U.S. and is still in existence today (Getter and Rowe 2006).

By the 1980s, Germany had a thriving green roof industry, inspiring the earliest research on green roof performance (Mentens et al. 2003). Widespread global adoption over the last two decades can be attributed to increasing environmental concerns, particularly in urban areas. With an estimated 40-50% of horizontal surfaces in cities occupied by roofs (Dunnett and Kingsbury 2004), governments have taken different strategies to drive green roof adoption. More countries are adopting regulations which are expected to accelerate green roof construction, such as France in 2015, which joined the numerous cities across the globe with legal requirements for green roofs such as Tokyo, Toronto, Copenhagen, and Zurich (Greenroofs.com 2015a). As of 2019, nine city governments have mandatory green roof requirements in the U.S. and 17 local governments have green roof incentive programs (GRHC 2019). Further, green roofs are

included as adopted technologies for in-situ stormwater management in numerous stormwater manuals across the country, including New York state (NYSDEC 2015). In 2015, over 17.5 million sq. ft. (1.63 million m^2) of green roofs are recorded in the industry projects database, with installations doubling since 2008 (Greenroofs.com 2015b; Lawson 2015). Industry analysis across North America estimates a 5-15% annual overall growth in green roof installations, with 3.1 million sq. ft. (288,000 m^2) installed in 2018 across 35 U.S. states and three Canadian provinces (GRHC 2019). Cited frequently for their co-benefits, green roofs contribute to the mitigation of urban heat islands (Alexandri and Jones 2008; Coutts et al. 2013; Takebayashi and Moriyama 2009), sequestration of CO_2 (Getter et al. 2009), increased biodiversity (Brenneisen 2006), urban stormwater management (Czemiel Berndtsson 2010; Speak et al. 2013; Villarreal and Bengtsson 2005), reductions in building energy consumption (Castleton et al. 2010; Jaffal et al. 2012), and increased roof life (Dunnett and Kingsbury 2004; Jaffal et al. 2012) among various other aesthetic and economic benefits (Jungels et al. 2013; Peng and Jim 2015).

1.2.1 Thermal Performance of Green Roofs

Green roofs can help regulate the thermal processes of the building envelope through evapotranspirational cooling, a change in albedo, shading, and a change in the thermal properties of the roof overall. Researchers in New York City found that on average a green roof daily peak membrane temperature in summer was 33°C cooler than a black roof peak membrane temperature (Gaffin et al. 2010). In an earlier study, the same researchers found the albedo of a green roof to be 0.2, while that of a maintained white roof was 0.7. They found that the albedo alone did not explain the thermal behavior of the roof, citing additional cooling on the green roof from latent heat loss (Gaffin et al. 2005). In Toronto, researchers found that average daily heat flow through a green roof was reduced 70-90% in the summer and 10-30% in the winter relative

to a traditional roof. Peak membrane temperatures were reduced by the green roof and were delayed by 5 hours relative to a traditional roof (Liu and Minro 2005). In addition to mitigating the urban heat island effect, lower ambient temperatures on roofs decrease air intake temperatures for HVAC systems, reducing building energy consumption during the cooling season (Wong et al. 2003a).

The selection of vegetation influences the rates of evapotranspiration and the albedo of the roof, but also contributes to the reduction of solar gain relative to a traditional roof due to vegetative surface shading (Jim and Tsang 2011; Pearlmutter and Rosenfeld 2008). The greater thermal mass of a green roof aids in stabilizing temperatures throughout the year. When constructing a new green roof over an older traditional roof, the thermal properties of existing insulation can influence the effect of adding the green roof on conditioning interior space. Researchers in Athens compared the impact of constructing a new green roof on buildings with different degrees of existing insulation. They found the contribution of the green roof on a highly insulated building to be small relative to a non-insulated building, with total energy savings of 2% compared with savings of 31-44%, respectively (Niachou et al. 2001). Other studies have also shown increased savings in non-insulated buildings over insulated buildings, leading to the conclusion that while green roofs can contribute to the overall building envelope performance, they should not replace insulation (Eumorfopoulou and Aravantinos 1998; Wong et al. 2003b). Further, studies on highly insulated buildings in warm climates have found that modern recommended levels of insulation ($R>4$ m^2 K W^{-1}) limit the ability of a green roof to influence interior temperatures, minimizing the benefits of passive cooling and shading (D'Orazio et al. 2012). On well-insulated buildings, the contribution of the insulation layers often minimizes the

contribution of multiple design choices, including vegetation and substrate types in green roof configurations (Zhao et al. 2013).

Regional climate influences green roof thermal performance. Modeling simulations show that for warm weather thermal performance, climates with higher water availability realize greater benefits through evapotranspiration and passive cooling relative to climates with lower water availability (Zhao et al. 2014). Few studies consider green roof thermal performance in cold winter climates (Getter et al. 2011; Liu and Baskaran 2003; Lundholm et al. 2014; Zhao et al. 2013), generally finding a modest thermal benefit of green roofs in cold weather, far lower than during warm weather conditions. Cold weather performance is additionally influenced by the accumulation of snow and its insulating properties. An early Canadian study found similar heat flux through a traditional roof and green roof after the accumulation of a snow layer (Liu and Baskaran 2003). In a plot study when comparing green and traditional roofs for two weeks in the winter, researchers found a 23% reduction in heat flux through the green roof relative to the reference roof in conditions with no snow cover. However, this difference was reduced to 5% with a snow layer. Surprisingly, the average mean heat loss by the green roofs increased with the snow layer, likely due to changes in weather between the two weeks studied, as acknowledged by the authors (Zhao et al. 2015). Even the roof microclimate and orientation, which strongly influence snow deposition and metamorphosis, can have a significant effect on winter thermal performance (Lundholm et al. 2014).

1.2.2 Hydrologic Performance

Increases in impervious urban land cover have altered natural hydrologic processes, overwhelming urban drainage systems during wet weather (NRC 2009a). This condition has resulted in occasional flooding with resultant loss of life and property (USEPA 2004). In

communities with combined sewer systems, the rapid runoff from impervious surfaces has led to the release of sewage to natural water bodies, which can damage ecosystems, known as Combined Sewer Overflow (CSO) (NRC 2009b). To reduce such problems, more regional treatment facilities, storage tanks, and other gray infrastructure have been constructed. These solutions are effective, but they are expensive, and they commit a community to use large amounts of energy and materials for the long-term future (USEPA 2004). Furthermore, gray infrastructure provides only one service, storm and wastewater management, and can negatively impact quality of life in urban neighborhoods.

Green roofs can reduce total stormwater flow into sewer systems, reduce peak flows, and delay stormwater entry into sewers—all of which can mitigate flooding and CSOs (Li and Babcock 2014). However, despite thousands of green roofs being constructed in cities around the world, our understanding of green roof performance in terms of these hydrologic functions is still far from complete.

Retention is the most commonly reported green roof performance metric in the literature (O'Connor et al. 2014; Fassman-Beck et al. 2013; Fioretti et al. 2010; Hakimdavar et al. 2014; Nawaz et al. 2015). Early studies in Germany between 1987 and 2003 found that extensive green roofs, those with substrate thickness less than 15 cm, retained between 27% and 81% of rainfall on an annual basis (Mentens et al. 2006). More recent studies have found volume retention for extensive roofs in the range of 15%–83% (Nawaz et al. 2015). Such wide ranges in performance are attributed to variation in the multiple factors which influence individual green roof performance, such as climatic patterns and roof design. The large variability in reported performance suggests that more research is needed to narrow anticipated performance of roofs based on design and climate parameters.

A high frequency of rain events and low evapotranspiration rates can result in poor green roof retention. Studies in the Pacific Northwest report low average event retention—12% –28% during their cool rainy winters (Schroll et al. 2011; Spolek 2008). In addition to retention, shape and layout of drainage systems on a roof can influence detention performance: by lengthening the flow pathway through the substrate or drainage layer, peak flow is reduced (Fassman-Beck et al. 2013; Hakimdavar et al. 2014). Study design also influences performance reported in the literature. Limited study duration and scale hinders the development of a complete understanding of the physical processes on the green roof.

The wide range of hydrologic performance reported in the literature results from a variety of factors, for example, study design, site design, and climatic conditions.

Study Design

Design of green roof studies influences the values for performance metrics reported in the literature. Many studies on green roofs have focused on the plot or test-box scale in an attempt to isolate specific design factors influencing performance. However, these studies do not explain performance on large-scale green roofs (Hakimdavar et al. 2014). Many of these plot-scale studies take place immediately following green roof construction and have 100% vegetative coverage (Speak et al. 2013), unlike full-scale roof applications. Further, studies with short duration may miss the impact of seasonal effects, both on precipitation patterns and roof performance.

Site Design

Green roof designs are often a balance between structural and financial restrictions and performance goals, such that a high range of variability in design exists. Design considerations

influencing performance include substrate depth and type, drainage layer depth and type, vegetation type and coverage, and slope (Olly et al. 2011; Seidl et al. 2011; VanWoert et al. 2005.; Wolf and Lundholm 2008). The retention performance of green roofs is a result of the potential water storage in the substrate. Some drainage layer designs also include depression storage, increasing the total storage. ET processes allow recovery of potential water storage following an event. Vegetation type and coverage influence ET rates, as larger vegetation with increased surface area intercepts more precipitation, and also has higher transpiration rates (Susca et al. 2011; Wong et al. 2003b). Roof age can also influence performance (Yang and Davidson 2021). In a Michigan study, researchers found that growth media organic content doubled over 5 years; this increase corresponded to a doubled porosity, and water retention that increased from an average of 17% to 67% (Getter et al. 2007).

Climate Conditions

Large variations in performance within studies are reported in recent literature (Carson et al. 2013; Fioretti et al. 2010; Nawaz et al. 2015; Palla et al. 2011; Stovin et al. 2012). This condition is believed to result from variation in natural precipitation patterns and the characteristics of individual precipitation events (Czemiel Berndtsson 2010). Examples of precipitation characteristics include total depth, duration, intensity, and event frequency (Hakimdavar et al. 2014; Speak et al. 2013; Stovin et al. 2013; Wong and Jim 2015; Zhang and Guo 2012). Event frequency, often measured as antecedent dry weather period (ADWP), aims to relate initial soil moisture conditions with performance metrics. Surprisingly, ADWP has been shown repeatedly to not have a strong relationship with performance, despite the importance of initial conditions. Given the complex processes governing ET during inter-event periods, ADWP does not consistently relate with initial soil moisture conditions, and thus cannot be used as a proxy for

initial soil moisture. However, a study in Hong Kong found that both solar radiation and wind speed influenced green roof performance (Wong and Jim 2015).

Statistical methods have been employed to identify the relationships among these factors, including single and multiple linear regression (Hakimdavar et al. 2014; Nawaz et al. 2015; Versini et al. 2015). The analyses are specific to region and site details, given the variety of influencing factors. As discussed below, these analyses have been used in a predictive capacity but function better in an explanatory capacity, providing insight into the strength of various parameters and their relationships to performance metrics (Wong and Jim 2015).

1.2.3 Stormwater Models

Research into stormwater management has considered both the stormwater quality and quantity impact of green roofs. Studies of green roof hydrologic modeling have a wide range in the literature from simple to complex (Li and Babcock 2014), though few of these studies consider the models that are frequently used by design professionals and required by regulators. Further, while results from empirical studies suggest variation in regional performance, Curve numbers (CN) and Runoff Coefficients (Cv) in the literature are not widely available (Fassman-Beck et al. 2016). Design professionals applying these methods rely on local jurisdictions to provide guidance on the appropriate CN and Cv for design, which are often rough estimates based on data from other locations. In larger jurisdictions, where available resources allow the development of guidance documents, justification for parameter selection is not commonly provided. This situation has created challenges for designers of green roofs.

1.3 Aims and Objectives

Green roofs are increasingly being adopted in cities around the world for their wide range of reported benefits. Yet despite this widespread adoption, research has yet to quantify the extent of the performance of green roofs, complicated by the variability in regional climate and roof design. Further, green roofs are integrated into stormwater management design in cities around the globe despite the lack of accurate ways to model their performance using methods applied by design professionals. This work aims to fill these critical gaps by quantifying the thermal and hydrologic performance of one green roof within its specific climate and calibrating model parameters commonly used in the practice of stormwater management.

1.4 Limitations

Inherently, as this work is limited to measurements on one extensive green roof, the results of this research describe only the performance of one roof in a single climate zone with one set of design parameters. Despite the use of duplicate instruments, signage, and security, there were times when the equipment failed, was inadvertently turned off, or was damaged and data were lost. While the study length exceeds that typically found in green roof literature, the hydrologic dataset excludes snowfall. In the Syracuse climate this is a significant portion (approximately one-third of the annual precipitation). Further, despite the relatively long study length for green roof research, only a handful of events exceed those used in design by practitioners. Statistically, seven 1-year 24-hour storm events would be expected, yet the data set developed as part of this research does not reflect that. This study also excludes consideration of any change in the green roof properties over time.

1.5 Structure

The research described in this thesis aims to address these questions by considering performance of one green roof in Syracuse, NY in Chapters 2 through 5. In Chapter 2 I describe the sensor network established on the roof beginning during its construction. In Chapter 3 I use simple thermocouple temperature sensors, installed at multiple layers throughout the roof, to quantify the contribution of each layer to the thermal activity on this part of the building envelope. In Chapter 4, I investigate the hydrologic cycle on the green roof using three years of data gathered on the roof. Finally, in Chapter 5 I expand upon the hydrologic performance documented in the previous chapter, extending the data set to seven years and comparing the performance of the two stormwater models most used by engineers in practice to model urban hydrology, namely the Curve Number Method and the Rational Method.

Chapter 2. Study site and Instrumentation

2.1 Study site

The site is located on the Nicholas J. Pirro Convention Center, part of the "OnCenter" complex owned by Onondaga County in Syracuse, New York (43.04368N, 76.14824W). Cold snowy winters and warm humid summers characterize the typical climate in Syracuse. Average seasonal temperatures and precipitation are given in Table 2.1. Approximately one-third of total annual precipitation falls as snow between the months of October and April, the majority of which is concentrated in the winter months (NCEI 2016).

Table 2.1. *Average climatic conditions from 1980 to 2015 by season in Syracuse, NY. Precipitation given is total precipitation (rainfall + snowfall) as equivalent water (NCEI 2016).*

	Average Temperature (°C)		Average Precipitation (cm)	Average Snowfall (cm)
	Minimum	Maximum		
Winter (12/1-2/28)	-7.4	1.1	19.8 ± 4.2	234
Spring (3/1-5/31)	2.2	13.6	23.8 ± 6.2	55.6
Summer (6/1-8/31)	14.9	26.5	27.1 ± 7.5	0
Fall (9/1-11/30)	5.5	16.7	27.1 ± 5.1	25.1

The green roof was retrofit onto the existing structure in 2011. The 5550 m^2 rectangular roof covers the ceiling of the main exhibit hall (Figure 2.1). The roof is sloped at −1% from the north–south centerline in both east and west directions. The roof's drainage structure includes drain conduits and a drainage mat below the substrate designed to convey excess water to the roof drains. Perforated triangular drain conduits, 5.1 cm in height, begin 5.1 meters from the centerline of the roof and run diagonally to each roof drain (Figure 2.2). There are 13 roof drains along the east side of the building and 12 along the west side. A gravel perimeter runs along the

Figure 2.1 *Looking south on the OnCenter green roof during the Summer 2013. The Belfort AEPG 1000 precipitation gauge and altershield are seen in the left side of the image while additional instrumentation on tripods is barely visible at the other end of the large roof.*

edge of the roof, including the area where the drains are located, accounting for approximately 1.7% of the total roof area.

A mineral-based substrate was sprayed onto the roof with an average 7.6 cm depth. Growth medium samples collected in 2011 were found to have an average organic content of 2.7% by mass. Analysis shows a relatively coarse composition, with 5.9% of the mass having a diameter less than 0.05 mm and an average bulk density of 0.79 $g \cdot cm^{-3}$ (Penn State University Agricultural Analytical Services Laboratory 2011). Lab measurements undertaken on substrate samples extracted from the roof in June 2016 found a porosity of 43% and a saturated hydraulic conductivity of 0.42 $cm \cdot s^{-1}$ (Yang and Davidson 2017). The substrate and drainage layer are underlain by a single ply waterproofing membrane and traditional roofing structure. Layers of roof construction are shown in Figure 2.3. Layers below the insulation and the insulation itself are original to the building and were not replaced during the retrofit. Material properties for layers of the roof are given in Table 2.2. Vegetation was established by spraying plant cuttings and covering them with a wind blanket designed decompose in part over time. Species of vegetation planted on the roof include *Sedum album*, *Sedum sexangulare*, *Sedum rupestre*, *Sedum floriferum*, *Sedum spurium,* and *Phedimus taksimense*.

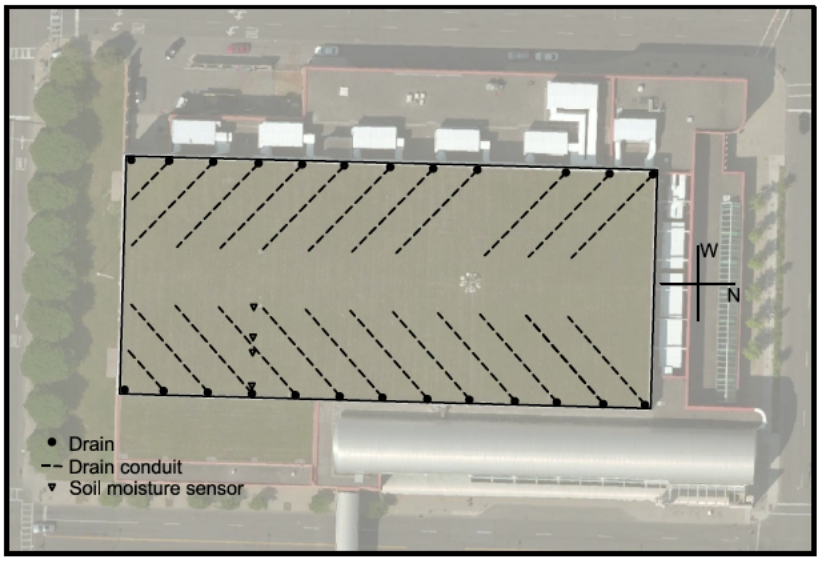

Figure 2.2 *Location of roof drains and drain conduits on the OnCenter green roof. Soil moisture sensors located along a transect on the eastern side of the roof are shown.*

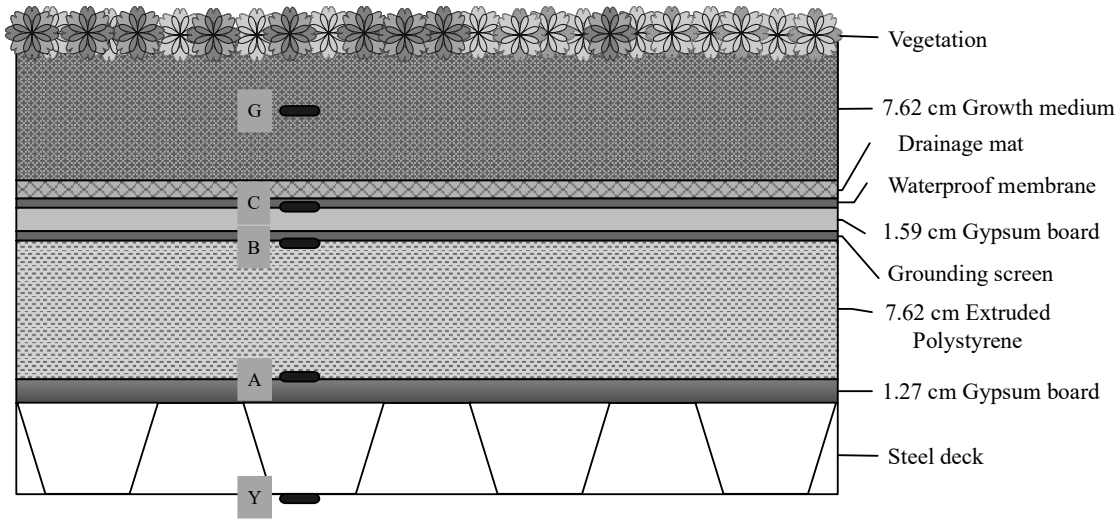

Figure 2.3 *Roof layers and temperature sensor locations within the OnCenter green roof.*

Table 2.2 *Thickness and manufacturer R-value of material layers. Only the bottom half of the growth medium layer is considered, since the temperature sensor is positioned in the middle of the layer. The R-value of the drainage mat is not known and is considered negligible.*

Layer	Thickness (cm)	Material R-value ($m^2K\,W^{-1}$)
Growth Medium	3.81	0.211
Drainage Mat	0.63	n/a
Waterproof Membrane	0.12	0.028
Gypsum Board 2	1.59	0.118
Grounding Screen	0.102	0
Extruded Polystyrene Insulation	7.62	2.64
Gypsum Board 1	1.27	0.079

2.2 Instrumentation

Temperature, soil moisture, rainfall, runoff, and ambient weather conditions are recorded using a CR1000 Datalogger and two AM 16/32B Multiplexers (Campbell Scientific, Logan, UT). Sensors used and reported accuracy ranges are given in Table 2.3 below. A rough schematic of sensor placement is provided in Figure 2.4. Additional information regarding detailed placement, installation, and calibration are given in the following sections.

Table 2.3 *Variables measured, sensors, and accuracy range for OnCenter green roof monitoring system. Accuracy listed for each sensor is taken from each corresponding instruction manual.*

Sensor	Variable measured	Accuracy
109	Temperature	±0.60°C (-50 to 70°C)
		±0.25°C (-10 to 70°C)
CS616	Volumetric Water Content	±2.5%VWC (0 to 50% VWC)
HMP155A	Relative Humidity	±1%RH (0-90% RH) (15 to 25°C)
		±1.7%RH (90-100% RH) (15 to 25°C)
		±(1+0.008 x reading) %RH (-20 to 40°C)
	Temperature	±(0.226-0.0028 x Temp) °C (-80 to 20°C)
		±(0.055 + 0.0057 x Temp) °C (20 to 60°C)
LI200x	Incoming Solar Radiation	±5% max (±3% typical)
03002	Wind Speed and Direction	±0.5 m s^{-1}
TE525	Rainfall	±1% (up to 1 in hr^{-1})
		+0, -3% (1 to 2 in hr^{-1})
		+0, -5% (2 to 3 in hr^{-1})
Belfort AEPG 1000		±0.25 mm

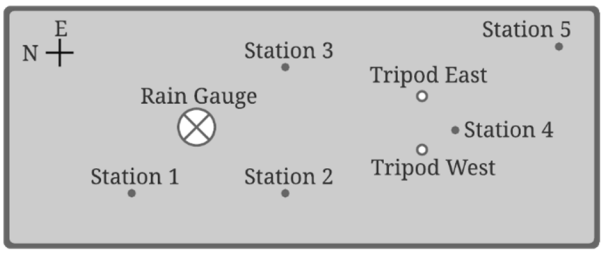

Figure 2.4 *Location of temperature profiles and equipment on the OnCenter green roof (111m by 50m).*

2.2.1 Temperature

Temperature sensors (109 Temperature Probe, Campbell Scientific) are installed in vertical profiles at five stations on the roof. Station locations were chosen based on construction schedule and were roughly evenly distributed across available space during installation. The positions of sensors at each station and the station locations across the roof are shown in Figure 2.3 and Figure **2.4**. Three temperature sensors, labeled Y, are mounted on the ceiling of the exhibit hall at stations 1, 2, and 5. Temperature sensors are scanned every minute and the data are averaged hourly. Interior temperatures are governed by an HVAC system that operates between two set points. These temperatures are further affected by the transfer of heat through the walls of the building, by high occupancy during events, by the physical partitioning of space during events, and by the opening of large garage doors along the west wall to enable access to the loading docks.

2.2.2 Soil moisture and sensor calibration

Soil moisture sensors (CS616, Campbell Scientific, Logan, UT) were installed along a transect, shown in Figure 2.2, to measure the change in soil moisture across the lateral distance of the roof. Sensors were buried midway through the substrate layer, 3.8 cm from the surface.

Sensors were calibrated following manufacturer specifications using site samples of substrate. The CS616 is a water content reflectometer (WCR) which consists of two parallel 30 cm-in-length stainless steel rods connected to an electronic measurement component. An electric pulse is generated and both this pulse and elapsed travel time of the pulse along the rods are used to determine the water content of the surrounding soil. In order to calibrate the sensors, multiple calibration boxes were built (35.6 cm x 11.4 cm x 10 cm) from clear PVC (Figure 2.5) and filled with growth media from the roof. Openings at 4.4 cm depth as measured from the bottom of the

box allowed for sensor placement at approximately midway through the depth of the substrate profile. After initial measurements are taken, 150 ml of water were added and the medium thoroughly mixed. This was defined as one interval and was repeated until the sample reached saturation. Finally, the media was dried at 55°C and the sample weighed. The quantity of water lost by drying is distributed equally across each interval and those weights used to determine the volumetric water content of the soil after each interval. The results of six trials and the calibration equation developed are shown in Figure 2.6. The equation determined via calibration (Equation 2.1) was sufficiently similar to the calibration equation provided by the manufacturer (Equation 2.2) that no adjustments were made based on this calibration.

$$\%VWC = (0.027 * Period - 0.408) * 100 \quad \text{Equation 2.1}$$

$$\%VWC = (0.0283 * Period - 0.4677) * 100 \quad \text{Equation 2.2}$$

Figure 2.5 *Water Content Reflectometer and constructed PVC box with substrate during calibration. An equal depth of substrate was added above the sensor prongs prior to calibration.*

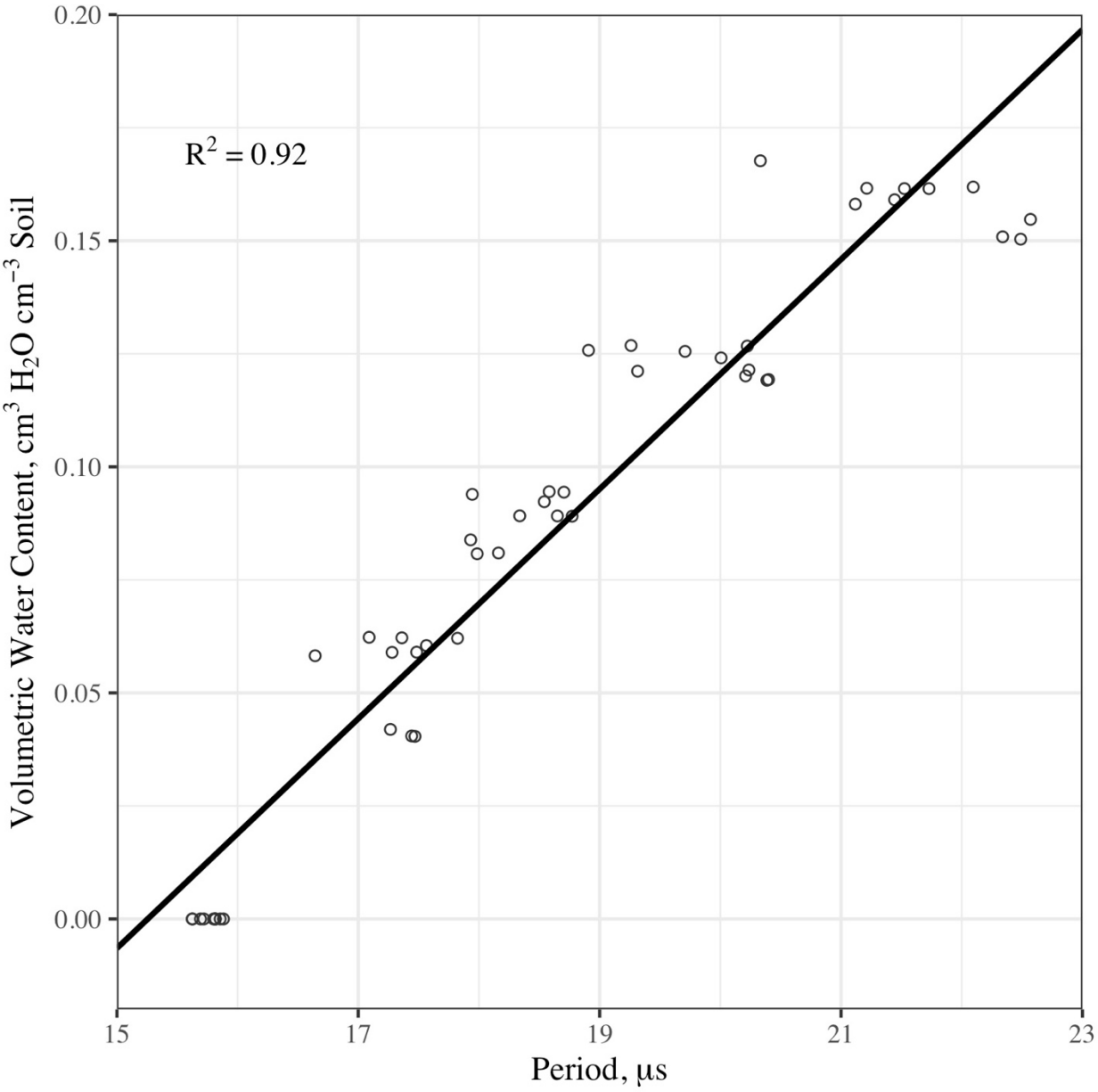

Figure 2.6 *Volumetric water content and period for multiple trials during soil moisture sensor calibration.*

2.2.3 Runoff and magmeter calibration

Roof runoff is collected from multiple roof drains and measured using electromagnetic flowmeters (M2000, Badger Meter, Milwaukee, WI). Electromagnetic flowmeters operate by inducing a voltage across a conductor, in accordance with Faraday's Law. The conductor in this case is the liquid which flows through the pipe. The flowmeter requires full-pipe conditions, so

pipes were configured in a way to ensure full-pipe (Figure 2.7). After removing a section of the existing 10-inch drainpipe along a horizontal run, a 10-inch x 4-inch wye was used to create a vertical drop while decreasing the diameter of the lower pipe. The magmeter was inserted in the lower pipe allowing for the required diameters of straight pipe before and after the meter. A 10-inch overflow bypass is configured above the 4-inch line, to comply with local code. Clear PVC was used for the straight runs of pipe used for both the 4-inch and the 10-inch lines, allowing for visual confirmation of both full-pipe conditions in the lower 4-inch pipe and a lack of flow in the 10-inch bypass.

Figure 2.7 *Magmeter pipe configuration prior to initial install. Pipe diameter was decreased from the existing 10-inch pipe (nominal pipe size, measured as inner diameter) to 4 inches. A 10-inch overflow bypass was maintained above the 4-inch line to comply with local code. No flow has ever been observed in the overflow pipe.*

A field calibration was performed on the first magmeter, which was used to collect data between October 2014 and June 2018 (Figure 2.8). Data presented in this work collected between January 2019 and April 2020 were collected using a second magmeter, the field calibration of which was performed by others and is not shown here. Both calibrations indicate that the factory calibration provided by the manufacturer was sufficient.

The field calibration occurred in December 2015 using a nutating disc flowmeter (Model 170, Badger Meter, Milwaukee, WI), using a water line previously run to the roof for irrigation purposes. Prior to turning on the water for each of the twelve trials, a baseline flow measurement was recorded from the magmeter to account for a minor amount of snowmelt observed to be occurring during the calibration. The water was then turned on and allowed to reach a stable flow, after which the flow rate was recorded from both the magmeter and the disc meter every minute for 5 to 6 minutes. The results of the twelve trials are summarized in Figure 2.8 below. Flowrates from pressurized flow quickly exceed that which is normally seen as runoff from the roof. The smallest flowrate recorded during the calibration was 0.22 L s^{-1}.

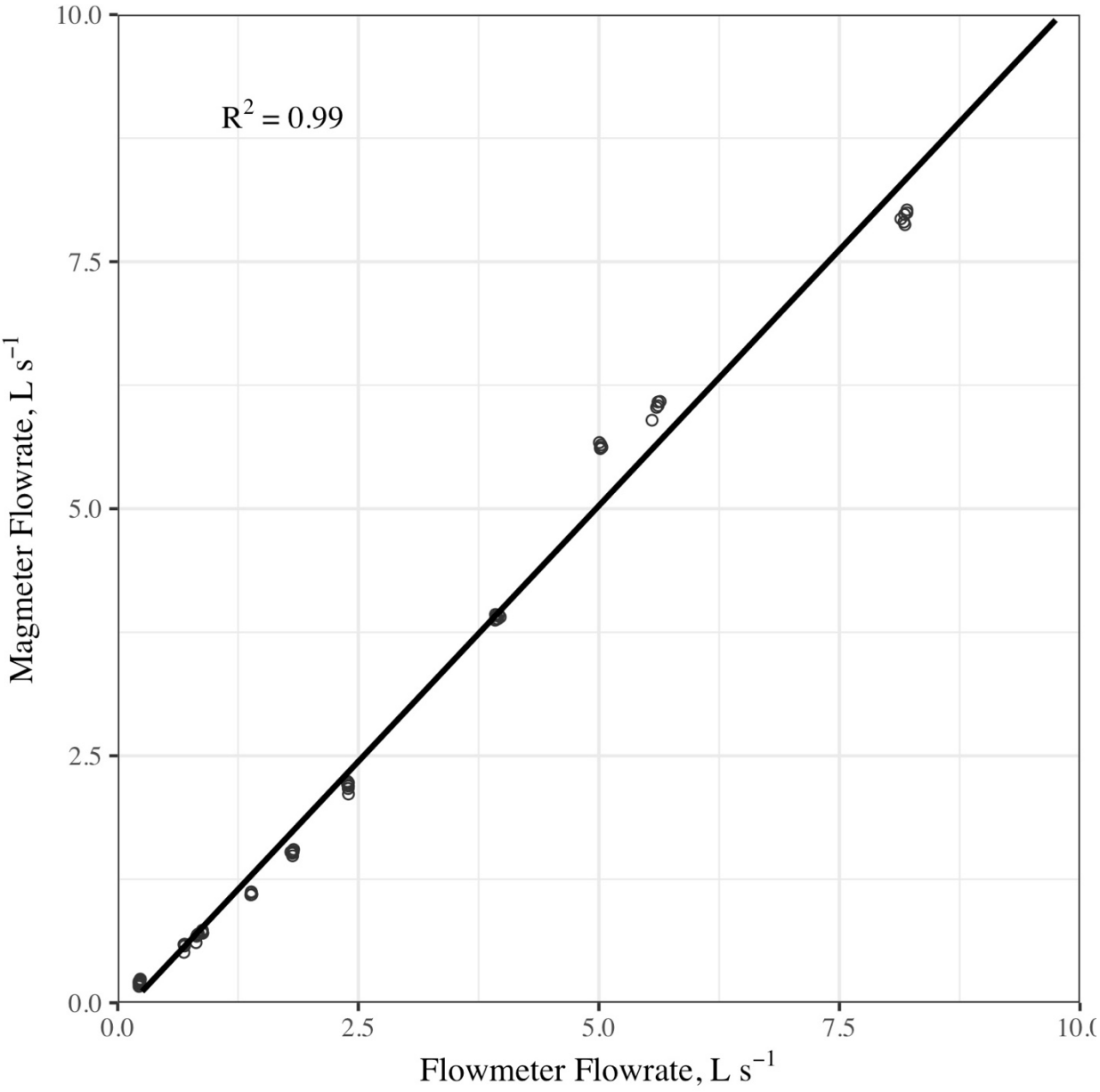

Figure 2.8 *Calibration curve developed from field calibration of an electromagnetic flowmeter using a nutating disc meter and a water source.*

2.2.4 Rainfall and weather

Campbell Scientific meteorological instruments include air temperature and relative humidity (HMP 155A), solar radiation (LI200X), wind speed and direction (03002), and precipitation (Tipping Bucket TE 525). These sensors are located on two tripods approximately

29 meters from the southern end of the roof, as shown in Figure 2.4. There is also a Belfort AEPG 1000 precipitation weighing gauge located 48 meters north of the two tripods.

Chapter 3. Heat flux and seasonal thermal performance of an extensive green roof[1]

3.1 Introduction

Thermal performance of green roofs and its influence on overall building energy use are heavily dependent on multiple factors including roof configuration and regional climate. Recent experimental work has focused on thermal processes over short periods or has attempted to quantify the influence of single components (i.e., vegetation) on the overall energy balance. Further, not all studies include detailed information on specific materials, despite the importance these play in roof performance (Castleton et al. 2010; Theodosiou et al. 2014).

The objectives of this study are as follows:

1) To provide measured and calculated thermal resistances of the green roof substrate and other roof materials and

2) To quantify the thermal performance of the green roof using measured temperature through multiple layers and net heat flux across the building envelope under summer and winter conditions in a Northeastern U.S. climate.

3.2 Methods

Under steady-state conditions sensors in layers A and B at each station can be used to determine the heat flow through the 7.62 cm insulation since its thermal resistance is known,

[1]Squier, M. and C. I. Davidson. 2016. "Heat flux and seasonal thermal performance of an extensive green roof." *Build Environ*, 107, 235-244. https://doi:10.1016/j.buildenv.2016.07.025.

similar to the method used by Gaffin et. al. (2010) on a roof in New York City. Quasi-steady state conditions were achieved during a period of significant snow accumulation on the roof. Substrate temperature has a linear relationship with heat flux and its constant value during this period is taken as confirmation of quasi-steady state conditions, shown in Figure 3.1. While temperatures in layer G are constant throughout most of February 2015, a storm on 2/14/15 resulted in damage to the datalogging system, and the loss of data for sensors 2 and 4 until the system could be repaired. Thus, only data from 2/1-2/14 are included in the calculation of heat flux. Station 3 is not included in the calculation of thermal resistance of winter temperature analysis due to sensor failure. This sensor was replaced in June 2015 and is included in summer temperature analysis.

The assumption of steady-state heat flow through the roof was used to apply Fourier's law to determine the thermal resistance of other layers.

$$q = \frac{1}{R}\Delta T \tag{3.1}$$

where q is the heat flux (W m-2), ΔT is the difference in temperature between two sensors (K), and R is the thermal resistance of the materials between the sensors (m2 K W^{-1}). R-values for adjacent roof layers can be summed to provide an overall thermal resistance for multiple layers.

3.3 Results & Discussion

3.3.1 Heat flux and thermal resistance

Thermal resistance is measured during winter after significant snowpack has accumulated on the roof, insulating the top layers of the roof. The temperature of the growth medium (layer G) is

given in Figure 3.1. Ambient temperatures measured above the green roof and snow depth taken from the Dewitt 1.4 WSW, NY weather station, located 4.1 km ESE of the study site are given in Figure 3.2 (National Operational Hydrologic Remote Sensing Center 2016). Manual snow depth measurements in late February 2015 showed depths mostly in the range 30-60 cm with a few locations having as little as 8 cm of snow. This uneven distribution is attributed to the redistribution and metamorphosis of snow after deposition.

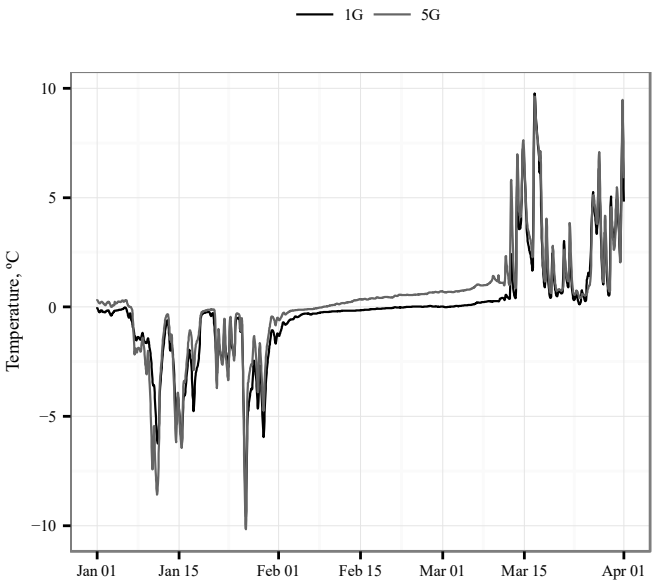

Figure 3.1 *Temperature in layer G at stations 1 and 5 during Winter 2015.*

Table 3.1 *Calculated R-values ($m^2K\ W^{-1}$) at four stations*

	5	1	4	2
B-C	0.245	0.170	0.180	0.268
C-G	0.216	0.306	0.218	0.241
Overall (A-G)	3.100	3.116	3.038	3.149

The average R-value of 3.1 $m^2 K W^{-1}$ is consistent with the range of 0.42-3.8 $m^2 K W^{-1}$ reported in the literature (Eumorfopoulou and Aravantinos 1998; Niachou et al. 2001; Wong et al. 2003a; b). The wide range results from the large variation in roof configurations. Increased soil depth supporting larger vegetation increases the overall R-value, as does any increase in insulation resistance. The largest contribution to the thermal resistance on this roof is the insulation layer (R=2.6 $m^2 K W^{-1}$). The contribution of the growth medium (and vegetation) to the overall thermal performance of the roof is small, which is consistent with studies on moderate to well-insulated roofs in other climates (Wong et al. 2003a). However, this roof is large relative to the other dimensions of the building, comprising a significant portion of the exposed surface area of the structure, so that even a small increase in thermal performance may be significant to the overall building energy performance. Within the analysis of individual layers on this roof, the magnitude of the R-value estimated for layer B-C is unexpected at nearly double the manufacturer's R-value for the Densdeck gypsum board.

3.3.2 Annual trends

The heat flux across the insulation layer is used as an indicator of the transfer of heat energy into or out of the building envelope. The daily average heat flux across this layer at all 5 stations from September 2014 – September 2015 is shown in Figure 3.3. On a daily basis the heat flux through the roof has a range of values, attributable to the diurnal cycle of temperature and solar radiation. These fluxes range from -5.76 Wm^{-2} in May to 9.46 Wm^{-2} in January. At the beginning of October daily fluxes are only briefly negative (downward), and by the end of October, fluxes remain positive (upward) throughout their daily cycle until mid-April. During the remainder of the year, late spring and summer months, the diurnal heat flux cycle experiences both negative and positive fluxes. The trends in fluxes entering and leaving the interior space are consistent

with the cooling and heating seasons. Net annual heat flux is estimated to be approximately 27 kWm^{-2}. The absolute magnitudes of the fluxes are larger than those reported in the recent literature, primarily due to different levels of thermal insulation and different regional climates (D'Orazio et al. 2012, Zhao et al. 2013).

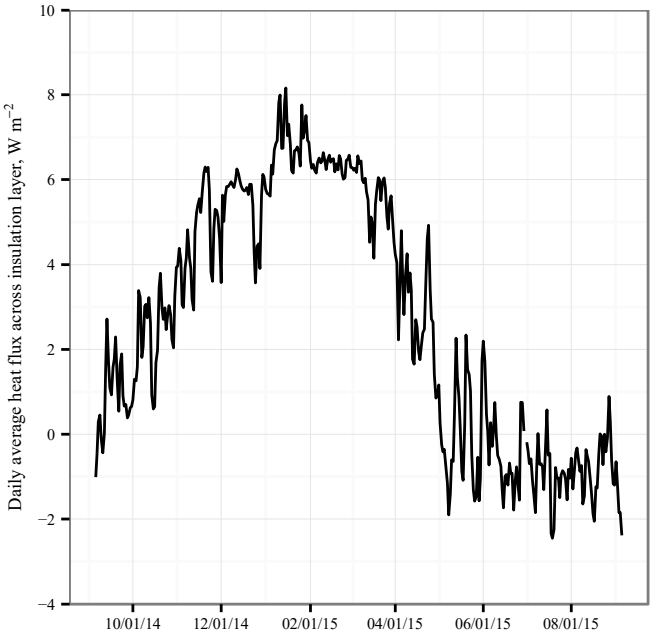

e

Figure 3.2 *Heat flux across the insulation layer from September 2014 – September 2015. Mean ± standard error for daily average heat flux shown is 2.71±0.75.*

3.3.3 Summer thermal behavior

Close to the summer solstice, Syracuse receives between 4 and 8 kWh m^{-2} total daily global horizontal irradiance (Renewable Resource Data Center). The average temperature calculated from all 5 stations for each layer for a period of 11 days characteristic of summer weather is shown in Figure 3.4. During dry weather in the summer months, a diurnal temperature cycle resulting from both exterior temperatures and high solar input is seen (6/24-6/26). The peak temperatures of the roof layers above the insulation (B, C, & G) are significantly larger than

those below the insulation (A & Y). In layers B, C, & G, both the maximum and minimum temperatures in each diurnal cycle are higher than the respective air temperatures for these three days. On 6/26, the warmest day in the subset shown, ambient temperature peaks at 25.8°C, while the average growth medium temperature reaches 33.3°C and the average membrane temperature (layer C) reaches 32.3°C. These membrane temperatures are higher than those reported in the literature for similar climates, probably due to variation in vegetation type and cover resulting in differing levels of reflected radiation and surface shading (Gaffin et al. 2010; Liu and Baskaran 2003).

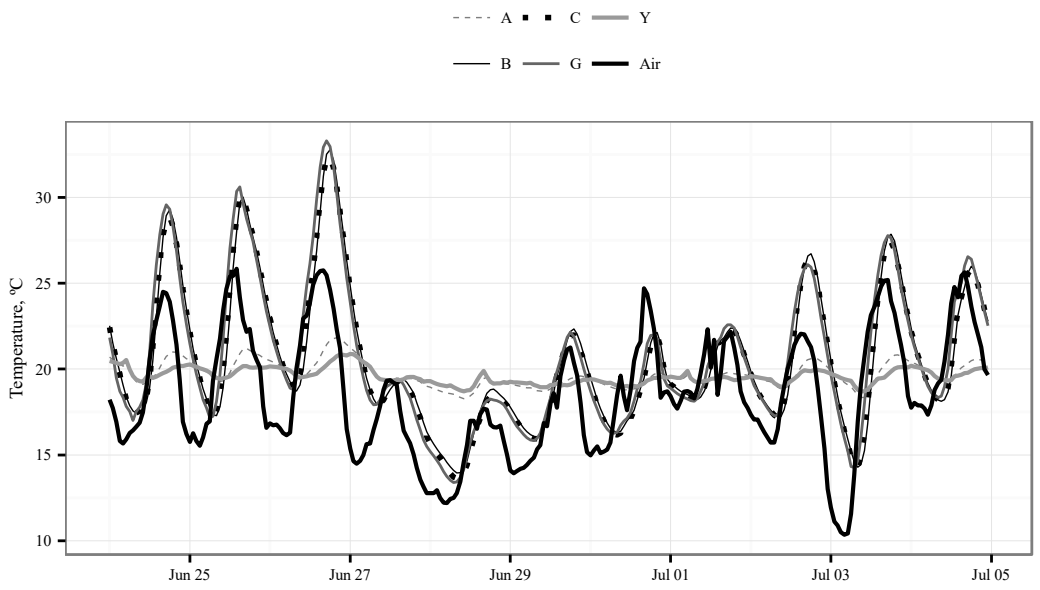

Figure 3.3 *Average temperature at each layer for all 5 stations during 11 days of Summer 2015. The curves for layer B and layer C are shown as a thin line and a sequence of dots, respectively, that are virtually identical to the curve for layer G. Standard deviations for the green roof layers range 0.46 to 4.01°C. Temperature for each layer with standard deviation is shown in Appendix A.*

During the day, the roof warms as the surface absorbs incoming solar radiation, which it re-radiates overnight into the atmosphere. The upper layers of the green roof release this heat at a

rate slow enough that the minimum temperatures never reach those of the surrounding environment. An overall decrease in amplitude in daily temperature cycles on the roof contributes to extended membrane life, as extreme temperature cycling is a lead cause of membrane failure (Dunnett and Kingsbury 2004). In contrast, during periods of low daily solar input (6/27-6/30 2015), temperatures are more similar to the ambient air temperatures of the period. Solar irradiance for the period is given in Figure 3.5. A series of precipitation events from 6/27-6/30 accompany the lower solar irradiance and leave the growth medium wet. While other studies have reported the significant contribution of passive cooling (Feng et al. 2010; Theodosiou 2003) and the change in thermal conductivity with changing soil moisture (Lundholm 2014) there is not enough evidence to determine the role evapotranspiration plays in cooling here. It is, however, clear that solar radiation plays a large role in heating the upper layers of the roof, and that this heating does not occur in the absence of significant solar radiation. Following the return of dry, sunny weather, the large amplitude diurnal trend returns. Fluxes across the period shown range from -5.4 to 2.1 Wm^{-2}.

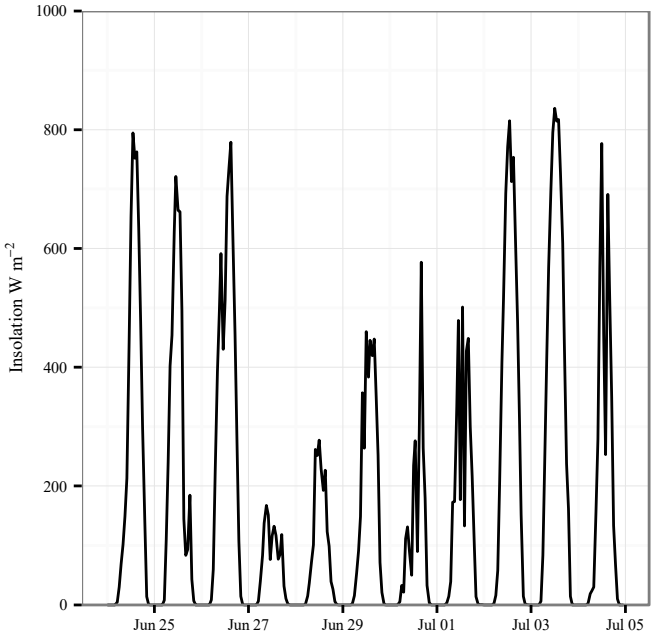

Figure 3.4 *Insolation during 11 days in June and July 2015.*

3.3.4 Winter thermal behavior

While most of the year the climate in Syracuse, NY could be described as cool, the winter months are characterized by occasional extreme cold and significant lake-effect snow. All of the days in the winter season (January to March) are heating days, with average ambient temperatures of -3.2°C. Average temperatures for all five stations for three weeks in January 2015 are shown in Figure 3.5, with the exception of layer G which does not include the sensor at station 3 due to sensor failure described in 3.2. The effect of the 7.62 cm insulation layer is seen in the large temperature difference between layer A and layer B. The diurnal pattern in layers Y and A is attributed to cycling of the building HVAC system as it heats the interior space. With low solar input during winter months, the flux of heat through the roof is driven by the temperature gradient between conditioned interior spaces and the ambient temperatures above the roof. The growth medium is generally above freezing during the winter season as other studies have reported (Lundholm et al. 2014). The extreme cold conditions resulting in freezing

temperatures in the growth medium during the three weeks shown in Figure 3.5 are an exception to this behavior. When snow covers the roof, the substrate temperatures (and thus heat fluxes) are relatively constant (Figure 3.1), consistent with other colder weather studies (Getter et al. 2011; Lundholm et al. 2014; Zhao et al. 2013). The influence of the accumulating snowpack (Figure 3.2) is visible in the increasing temporal lags in maxima between the growth medium and the air temperature as snow accumulated on the roof, ranging from 6 to 30 hours in January. Fluxes across the period shown range from 4.5 to 9.5 Wm^{-2}.

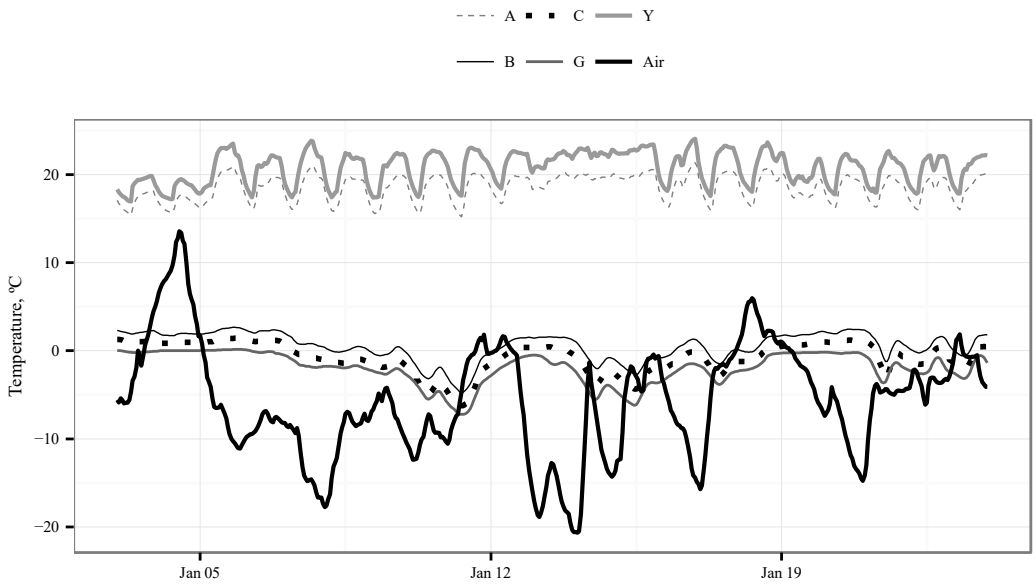

Figure 3.5 *Average temperature at each layer during 19 days of Winter. Standard deviations for the green roof layers range 1.46 to 1.83°C. Temperature for each layer with standard deviation is shown in Appendix A.*

3.4 Conclusion

In this study, a monitoring campaign was undertaken to further understand the thermal performance of an extensive green roof and the influence of time of year on this performance. The green roof contributes to reduction in heat transfer across the building envelope, but the thermal resistance provided by the insulation layer limits its overall contribution. During summer months total daily solar input is highest and drives downward (negative) heat fluxes through the roof. Outside of this high total daily solar input, the heat flux through the roof is generally upward (positive). During winter months an accumulated snow layer behaves as an insulating layer on the roof, thermally isolating the green roof from ambient weather. During this period the green roof reaches a quasi-steady state and material thermal properties can be measured. These material properties generally agree with those reported in the literature and by manufacturers, except for an area where it appears that a grounding screen allowed for trapped air. These results demonstrate the importance of measuring and reporting material properties for all layers of the roof when the entire roof is considered. Future work should consider the contribution of the various layers to the thermal efficiency of the building envelope, particularly in milder climates with less traditional insulation.

Chapter 4. Hydrologic performance of an extensive green roof in Syracuse, NY[2]

4.1 Introduction

Green roofs are one type of green infrastructure technology applied globally as part of a modern approach to stormwater management. The addition of growth media and vegetation creates additional water storage on the roof (pore spaces) and a new pathway for water to leave the roof (plant uptake and transpiration) (O'Connor et al. 2014; Fassman-Beck et al. 2013; Hakimdavar et al. 2014; Nawaz et al. 2015). Further, water stored in pore spaces has more opportunity to evaporate from the roof, providing recharge of the available storage space (Fioretti et al. 2010; Wong and Jim 2014). All of this prevents water from reaching the storm sewer, helping to mitigate flash flooding in urban areas. The additional material on the roof also increases the length of the flow path for water that is not retained, increasing the detention time (Hakimdavar et al. 2014; Carson et al. 2013; Johannessen et al. 2018). Both metrics are documented in the literature, however, as explained in Chapter 1, many differences in study design, site design, and climate result in a wide variety of reported results.

In this study I take advantage of year-round monitoring on a large extensive green roof with an integrated drainage structure in Northeast U.S. to accomplish two goals: (1) to quantify detention and retention performance under a variety of weather conditions, and (2) to identify the dominant hydrologic processes driving performance. To do this, rainfall, runoff, soil moisture, and meteorological data have been collected over 21 months from a full-scale green roof in

[2]Squier-Babcock, M. and C. I. Davidson. 2020. "Hydrologic performance of an extensive green roof system in Syracuse, NY." *Water-SUI*, 12, 1–18. https://doi:10.3390/w12061535.

Syracuse, New York. The data are used to identify 165 rainfall events for which various hydrologic parameters are quantified. The rainfall record is first placed in an historic regional context (between 1950 and 2010) to support interpretation of study results across longer periods. Hydrologic performance on the roof is then considered using common performance metrics.

4.2 Methods

Data reported here are collected between October 14, 2014 and July 8, 2016. Meteorological data are measured at hourly intervals. Hydrologic data are measured at 15-minute intervals between October 2014 and April 2015, after which they are measured at 5-minute intervals.

4.3 Data analysis

4.3.1 Event analysis

Continuous event data were sequenced using the eventseq function from the Hydromad package in R (Andrews and Guillaume 2016) using the following criteria:

1) no precipitation for 6 hours prior to the start of an event, and

2) runoff from any previous events must have ceased prior to the start of an event.

In addition, days where snow was falling and days with visible accumulated snow on the roof were eliminated from the dataset. These days were identified using records collected by NOAA at the Syracuse Hancock International Airport (NCEI 2016). Of the 634 days included in the study period, 177 were eliminated by the snow criteria, and 72 events occurring on these days were removed. Six additional events were removed due to flowmeter failure as a result of vandalism. Buried soil moisture sensors were found to migrate upwards slightly during the

winter. While soil moisture is reported for events in 2016, the sensors may not have been measuring at the same depth as previous events.

Descriptive parameters considered in the study include rainfall depth (RD), runoff depth (RuD), and initial soil moisture, measured as volumetric water content (aVWC). In lieu of reporting antecedent dry weather period (ADWP), soil moisture is reported for the time-step preceding the start of an event. While ADWP has in the past been used as a proxy for substrate conditions at the onset of an event (Razzaghmanesh et al. 2014; Stovin 2010; Wong and Jim 2014), recovery of the substrate between rain events is complex and an exclusive relationship between the two does not exist (Hakimdavar et al. 2014; Nawaz et al. 2015; Van Spengen 2010).

Common retention and detention metrics are used to quantify performance (Figure 4.1). For the purposes of comparison, rainfall and runoff are expressed as equivalent depth in mm. Events are furthered categorized by event size, adapted from classifications previously reported in the literature (Wong and Jim 2014; Carson et al. 2013). Meteorological seasons are used for seasonal analysis.

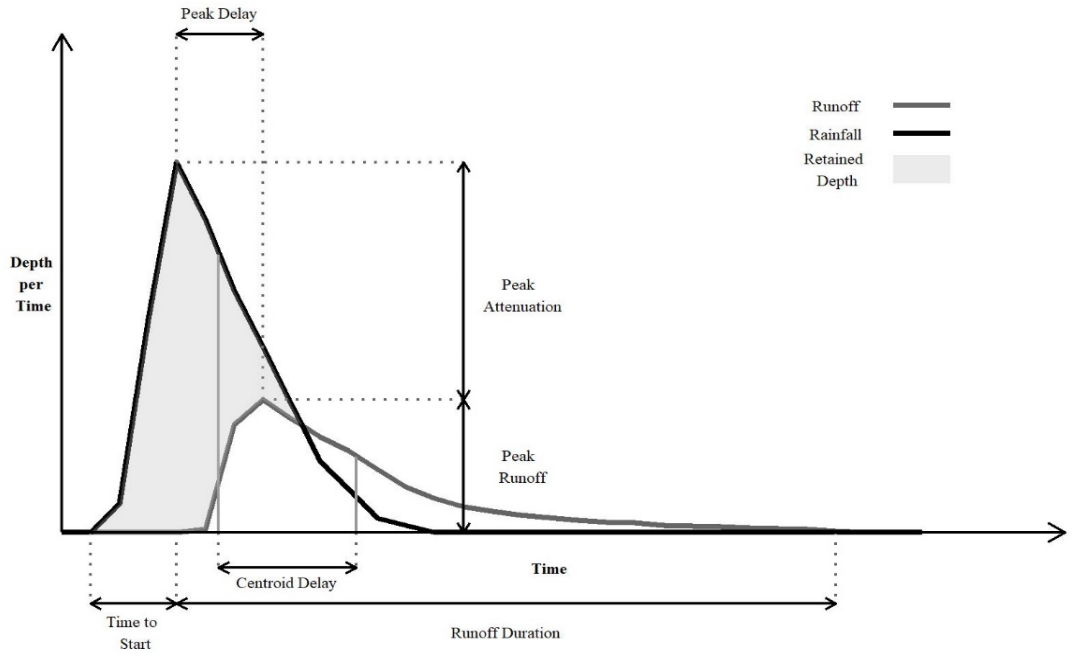

Figure 4.1 *Conceptual diagram of rainfall and runoff showing retention and detention metrics.*

4.3.2 Event plot statistical analysis

To identify the influence of season on runoff behavior, a one-way ANCOVA was conducted to determine whether a statistically significant difference exists between seasons based on exceedance probability controlling for runoff data. Runoff data are transformed as log(n+1) to include zero value events and meet the requirements of normality.

4.3.3 Evapotranspiration analysis

Evapotranspiration (ET) is quantified using a mass balance approach for hourly data collected between April 25, 2015 and July 8, 2016, following Equation 4.1:

$$P - RO - ET = \Delta S \tag{4.1}$$

where P is precipitation, RO is runoff, ET is evapotranspiration, and ΔS is change in soil moisture, all expressed in mm hr^{-1}. Steady state conditions are necessary for this approach, which under real-world conditions requires P = RO = 0 at the site. Additionally, sensor reliability issues for potentially frozen substrate require the removal of all days where temperature in the substrate is at or below 0°C. Days with the potential for snowpack are removed due to complex mechanisms of snowmelt and unknown conditions within the substrate. Daily change in soil moisture is taken as the difference between the hourly values recorded at 0:00 and 23:00 for each day meeting the above conditions. The daily ET is averaged across the four soil moisture sensor locations.

4.3.4 Weather during the study period

Weather during the study period was generally consistent with historic temperatures (Figure 4.2). Total precipitation in the region was higher than the historic regional precipitation for 9 of the 21 months in the study period. A total of 1062 mm of rainfall were measured at the site during this period, excluding snow events. Measured total precipitation averaged over 1950-2010 at the Syracuse Hancock International Airport, located 8.3 km north of the OnCenter, is compared with the rainfall measurements taken at the OnCenter between November 2014 and May 2016 (Figure 4.3). Daily total rainfall during these periods is comparable, with reasonable differences attributed to the spatial variability of rainfall.

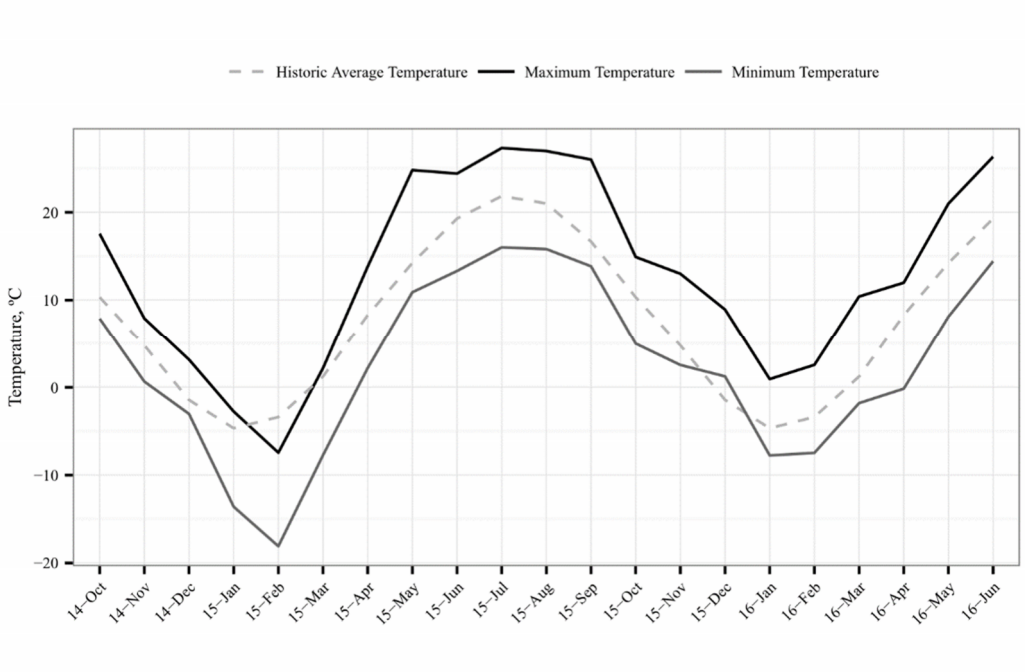

Figure 4.2 *Historic temperatures as recorded from 1950-2010 at the Syracuse International Airport and actual temperatures measured on the OnCenter green roof from October 2014 to July 2016 (NCEI 2016).*

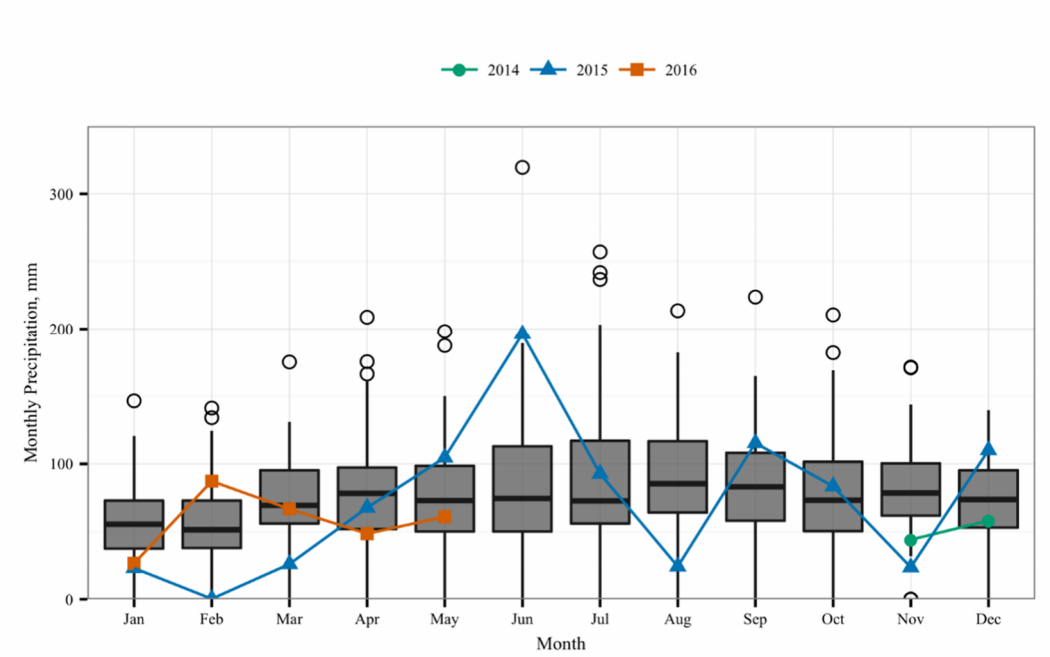

Figure 4.3 *Tukey box and whiskers plots for the monthly historical precipitation from 1950-2010 as recorded at the Syracuse Hancock International Airport (NCEI 2016). The bottom and top of the box represent the first and third quartiles, and the band inside the box represents the median; whiskers are presented in the style of Tukey (Tukey 1977; McGill et al. 1978; Wickham 2016). Data not included in the whiskers are plotted as outliers. Monthly rainfall as recorded at the OnCenter green roof between November 2014 and May 2016 are reported as colored lines. Snow is not included in monthly totals at the OnCenter green roof but is included in the historic averages recorded at the airport. Months where rainfall is recorded for only part of the month (Oct-14, Jun-16) are included in the monitoring period but are not included on this plot.*

Following removal of the non-qualifying events, 165 events remain. Rainfall duration and depth for each event are given in Figure 4.4 overlain by updated recurrence intervals for the region based on historic precipitation records through 2008 (NRC-NRCC 2016). Of these events, 3 exceed the 1-year recurrence interval, one of which nears 5-year recurrence. Despite the high frequency of events, the 84 very small (< 2 mm) events comprise only 5% of the measured rainfall during the study period. The 11 large events (> 20 mm), however, account for 38% of the total rainfall measured. It is important to note that the green roof was designed to hold a 25.4 mm rain event.

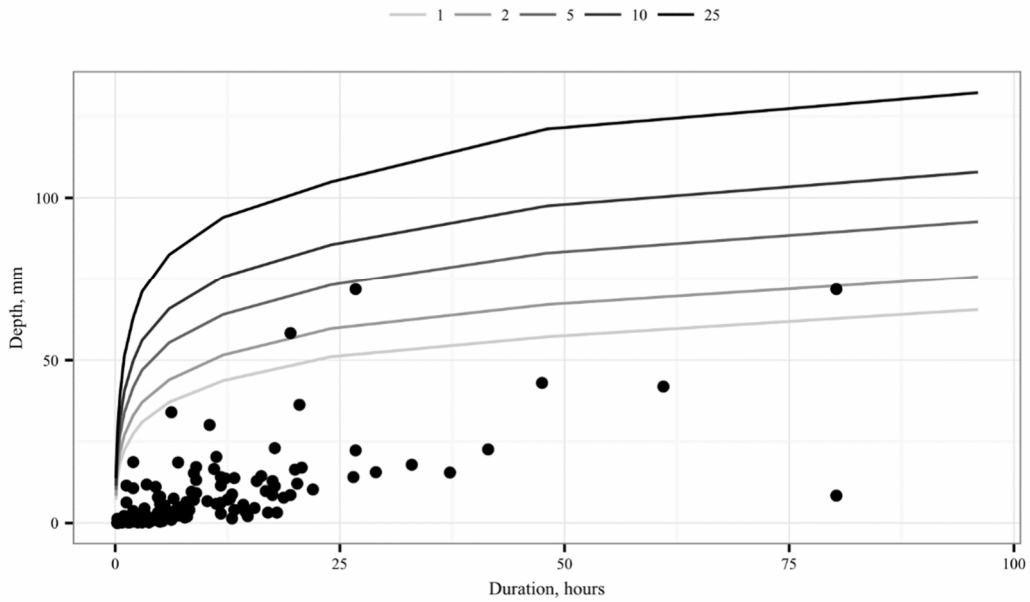

Figure 4.4 *Rainfall duration and depth with recurrence intervals in years for Syracuse, New York. Recurrence intervals are based on historic data measured between 1950 and 2008 for the region (NRC-NRCC 2016).*

4.4 Results and Discussion

4.4.1 Green roof performance

Cumulative retention, defined as rainfall minus runoff, on the green roof is 56% over the study period, a total retained depth of 599 mm. Given the 5550 m^2 roof area, a total of 3350 m^3 of rainfall is retained during the study period. Full capture, where no runoff is observed, occurred for 106 events, or 64% of the events. Overall mean event retention is 85%. Nawaz et al. (2015) found that cumulative retention for 19 studies varied widely, between 15 and 83%, with average and median retentions of 57% and 59% respectively. One experimental study in New York City found a 55% cumulative retention during their study period for a roof with a 25.4 mm growth medium depth (Abualfaraj et al. 2018). Studies with growth media of similar depth to the study (70-100 mm) reported overall mean event retention between 52 and 74% (Carson et al. 2013; Hathaway et al. 2008; Kurtz 2008; Liu and Minor 2005; Voyde et al. 2010), though comparison

to other studies has limited value as many factors influence the performance of individual roofs. Note that three of the above-mentioned studies are also cited by Nawaz et al. (Carson et al. 2013; Hathaway et al. 2008; Voyde et al. 2010). In contrast, a study in Norway reported an annual retention of 11-30% across multiple green roofs including both rain and snow, with a higher 22 – 46% reported between May and October for rain only (Johannessen et al. 2018). On ten plot-scale green roofs, Liu et al. found mean event retention between 23 and 33.2% (Liu and Chui 2019). Significant variation exists across experimental studies reported in the literature, and recent studies have begun to consider the influence of multiple factors on the reported performance (Gong et al. 2018).

Detention metrics, summarized in Table 4.1, are calculated for the 39 events where 5-minute data are available and runoff occurred. Peak attenuation ranges from 0.11 to 5.2 mm/5-min with an average of 1.3 mm/5-min. Runoff delay is calculated from peak to peak and centroid to centroid.

Table 4.1 *Detention metrics for 39 events where runoff occurred, and data is collected at the 5-minute timestep. A visual definition of detention metrics is given in Figure 4.1.*

Metric	Minimum	Maximum	Average	Median
Peak Delay, hours	-0.92	30	3.3	0.75
Centroid Delay, hours	0.18	17	3.2	2.5
Peak Attenuation, mm/5-min	0.11	5.2	1.3	0.68
Peak Runoff, mm/5-min	0.01	1.4	0.31	0.26
Time-to-Start, hours	0	12	3.6	2.8
Runoff Duration, hours	0.5	48	13	11

The peak delay, calculated for the 5-minute timestep, ranges from -0.92 to 30 hours, with a mean and median of 3.3 and 0.75 hours, respectively. Despite the wide range, most events have a short delay, with 71% falling between 0 and 2 hours. Only one event had a negative delay. The

peak in runoff occurring prior to the peak in rainfall is a result of the natural variability of rainfall during an event and calls into question the appropriateness of the peak delay metric. In contrast, the centroid delay for this event is 1.5 hours, demonstrating that the center of the rainfall event still preceded the center of the runoff event. One long event with a 30-hour delay had 41.9 mm of rainfall over 61 hours, with most of the rainfall occurring in the first few hours of the event. The green roof growth media had the capacity to retain almost all of the first few hours of rainfall. However, the event continued at a slower rate until the capacity of the roof was exceeded and some runoff occurred, with only 63% of the total event being retained. Both of these peak delays are a result of the temporal variability of rainfall within an event and the time scale over which the roof responds. Peak delay, among other detention metrics used in green roof research, is borrowed from the field of hydrology where response times on a watershed scale are considerably longer. Other researchers have found similar behavior and also question whether the peak delay provides an accurate inter-event comparison (Sims et al. 2019; Stovin et al. 2012; Stovin et al. 2017).

The delay between the onset of rainfall and runoff is, in part, a product of the antecedent soil moisture which will be discussed in the Section 4.4.2.3. As rainfall continues, the retention capacity of the substrate is exceeded, and runoff begins. The wide range of detention metrics results from the temporal patterns of precipitation within an event and the initial conditions of the substrate which also influence retention. Detention metrics cannot be separated from initial losses. After moisture within the substrate exceeds field capacity, runoff response is quick and predictable. Each peak in precipitation is followed by a corresponding peak in runoff, not unlike a small watershed whose runoff is strongly governed by hill-slope mechanics (Dingman 2002).

The time response of the green roof results in multiple peaks within a single event definition. Previous observations on a plot-scale suggest runoff will follow rainfall almost immediately after the retention capacity of the roof is exceeded (Stovin et al. 2012). Observations on this full-scale roof suggest a delay of 15 minutes after the retention capacity of the substrate is met, though some of this may be attributed to the time required to travel the distance between the roof drain and the in-line flowmeter and to the equipment measurement interval. Further, this roof design incorporated drain conduits across the roof, as shown in Figure 2.2. As the designers intended these drain conduits aid in the removal of excess water from the growth medium, decreasing the detention time during large events.

4.4.1.1 Performance by event size

The largest events are responsible for a smaller portion of overall retention, while most of the rain falling as small and very small events is retained, shown in Figure 4.5. Only one event less than 2 mm experienced any runoff. This event generated 0.03 mm of runoff from 0.65 mm of rainfall occurring on already very wet substrate (aVWC = 0.20). The event occurred just outside the 6-hour event definition allowing it to be separated from the previous event. Only 24% of the measured retention occurred within the 11 large events, detailed in Table 4.2. Further discussion of the effect of aVWC on evapotranspiration is included in Section 4.3.3.

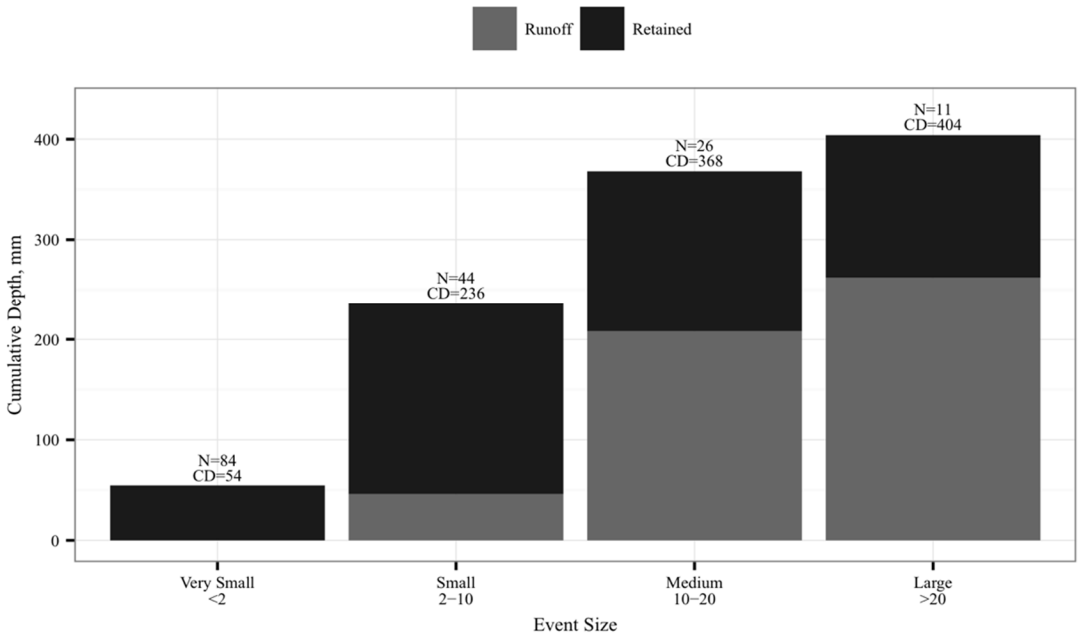

Figure 4.5 *Runoff and retention from the OnCenter green roof, designed to hold a 25.4 mm rainfall event, grouped by event size. Cumulative depth (CD) is the sum of runoff and retained depth. Total rainfall over the 21-month study period, excluding snow days, is the sum of cumulative depths in each range, 1062 mm in total.*

Table 4.2 *Details for 11 events which exceed 20 mm in total depth. Retention depth is calculated as the difference between rainfall and runoff depth. Initial soil moisture is the average of the four sensors the timestep preceding the onset of rain.*

Start Date and Time	Rain Depth, mm	Retention Depth, mm	Initial Soil Moisture, m^3 m^{-3}
Oct 15, 2014 11:15	36.3	7.46	0.084
May 18, 2015 17:00	34	17.3	0.038
May 30, 2015 17:30	41.9	26.4	0.019
June 14, 2015 16:30	20.3	8.15	0.120
June 27, 2015 14:00	43	23.5	0.040
June 30, 2015 19:45	58.3	0.615	0.148
Sept 29, 2015 11:00	71.8	16.1	0.040
Oct 9, 2015 1:45	23	12.3	0.075
Dec 1, 2015 23:15	22.3	3.16	0.157
Dec 29, 2015 11:45	22.6	3.9	0.158
May 29, 2016 13:30	30.1	23.1	0.017

4.4.1.2 Performance by season

Event average retention is lowest during the winter and not substantially different in the remaining seasons, shown in Table 4.3. Cumulative seasonal retention is highest in the fall and spring and lowest in the winter. Lower retention during the winter is explained by lower rates of evapotranspiration during inter-event recovery periods. Climatic conditions during the summer months, however, promote the highest rates of evapotranspiration, which should result in high overall retention in the absence of other influencing factors. Yet summer cumulative retention is only 35%, lower than both the fall and spring. Rainfall patterns vary with the season. Summer has both less rain events and higher average event intensities than the spring or fall. During the study period, rainfall for the months of May, June, and July is higher than the median historical data. The average event peak intensity during the summer exceeds 8 mm hr^{-1} while the next highest, during the spring, does not exceed 5 mm hr^{-1}. It appears that the higher intensity, lower

frequency rainfall patterns experienced during the summer contribute to the season's lower performance.

Probabilities of exceedance for runoff depth separated by season are given in Figure 4.6. Winter events are more likely to result in greater runoff depth, consistent with the behavior reported in the literature (Carson et al. 2013; Elliott et al. 2016), and the low average retention for this season. The results of a one-way ANCOVA found that the difference in runoff behavior is statistically significant at the 0.05 level only for winter and summer. Weather conditions between the spring and fall are not statistically different, but an increase in the number of events in future data collection periods along with consideration of other weather factors may provide more insight into these trends.

Table 4.3 *Retention by season for the OnCenter green roof.*

	Seasonal Retention		Rainfall	Event Count		Average Intensity	
	Event average, %	Cumulative, mm	Depth, mm	Full capture	Total	Event mean, mm hr^{-1}	Event peak, mm hr^{-1}
Fall	89.2	141	310	34	52	0.654	4.12
Winter	70.1	44.5	158	12	25	0.479	2.45
Spring	88.7	160	329	36	53	0.525	4.92
Summer	85.3	93	265	24	35	1.01	8.17

4.4.1.3 Evapotranspiration

Retention performance has an inverse relationship with aVWC. The substrate has a finite capacity to hold water, after which all incoming precipitation enters the drainage structure. The difference between the soil moisture level in the substrate and its maximum capacity is the available water retention capacity. During inter-event periods the retention capacity of the substrate is restored via ET.

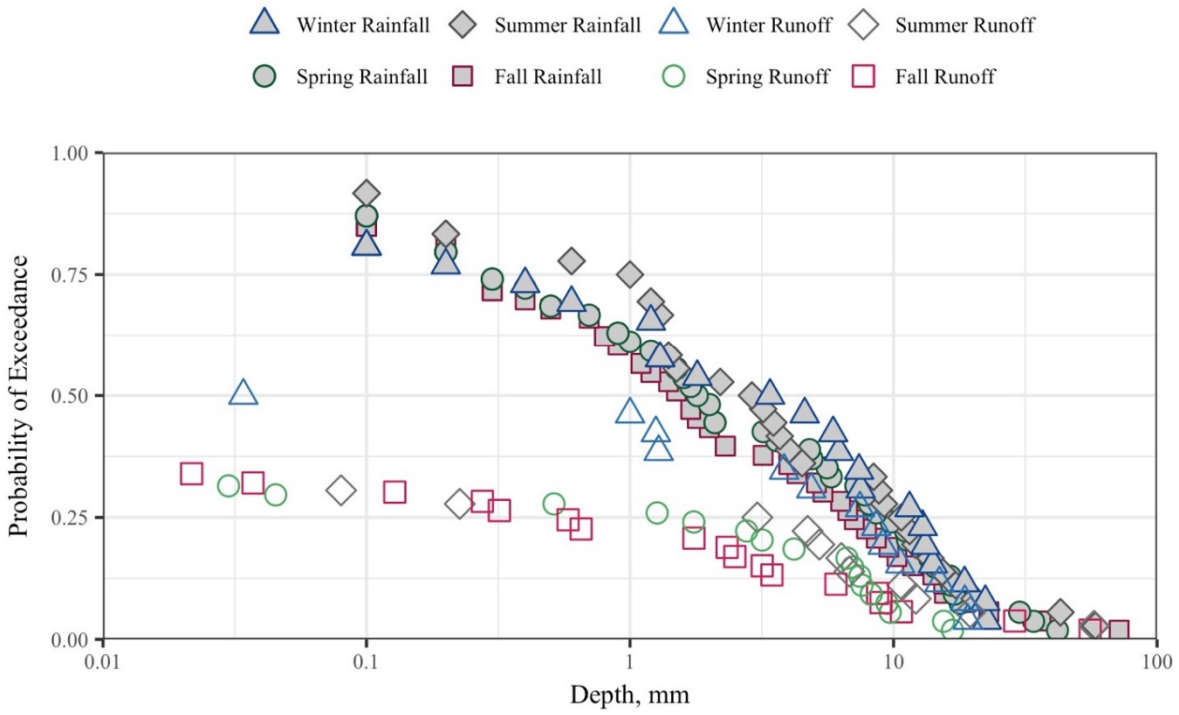

Figure 4.6 *Event exceedance probability for runoff depth separated by season for the OnCenter green roof.*

Daily ET rates for dry days averaged across a transect of the roof, shown in Figure 4.7, range from 0 to 2.5 mm day^{-1}. On this same roof, daily ET measurements for both wet and dry days during warm months (May, June, July, and August) between 2015 and 2017 are found to range from 0-5.4 mm day^{-1}, with a daily average of 0.76 (Yang and Davidson 2020). Plot scale studies planted with S. mexicanum and D. australe in New Zealand found ET rates from 1.9-2.2 mm day^{-1} under unstressed water conditions (Voyde et al. 2010). Measurements made on two green roofs in New York City in 2009 and 2013 found average daily ET of 0.24 mm day^{-1} and 0.72 mm day^{-1} in December and 4.80 mm day^{-1} and 4.94 mm day^{-1} in July (Marasco et al. 2014). The ET measurements here are within these ranges measured on other roofs. Differences between measurements made in Syracuse and New York City may result from differences in

weather as well as in roof construction, i.e., substrate retention properties. A consistent drying curve for ET is visible for multiple periods throughout the data set as a series of points decreasing in a nearly vertical line. A longer dry period results in a nearly vertical line with slight curvature near the bottom of the graph, due to decreasing ET as the soil dries, e.g., between April 25 and May 9, 2015, as available soil moisture has a direct relationship with rates of ET. As weather cools through the Fall 2015 and the available energy for ET decreases, there are fewer points with large ET. The current method of estimating ET cannot be used with snowstorms, but there are some rains in December and February which enable estimates of ET that are less than 1 mm day^{-1}. Rising temperatures in March, April, and May result in increasing maximum values of ET. Between late May and early July infrequent and intense storms result in high ET rates immediately following an event and long consistent decay in June - July 2016.

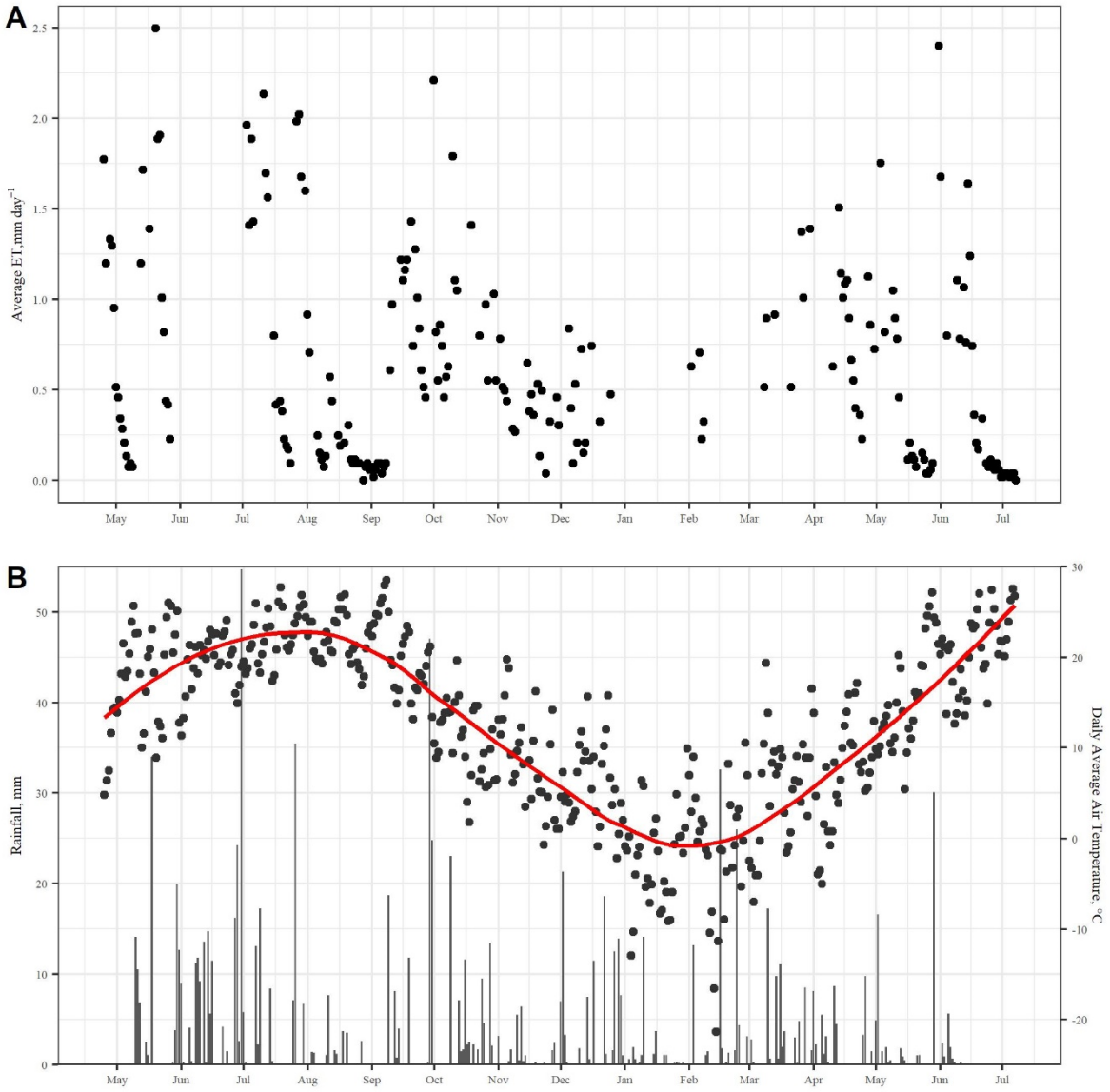

Figure 4.7 *(A) Average evapotranspiration as quantified on the OnCenter green roof for dry days between April 25, 2015 and July 8, 2016. (B) Daily average temperature with a local linear regression and daily rainfall as measured on the OnCenter green roof between April 25, 2015 and July 8, 2016.*

ET rates are limited by the availability of energy and water. Daily maximum insolation and initial daily soil moisture are considered relative to daily ET rates as proxies for available energy and water on the roof, shown in Figure 4.8 and Figure 4.9, respectively. As insolation increases, the maximum ET rates (corresponding to sunny days) show a roughly increasing pattern. Days

with low maximum insolation, less than 250 W m^{-2}, are cold weather days in late November - December 2015, where lower ambient temperatures also contribute to the low ET rates. While cloudy summer days are included in the study, all days between October 27, 2015 and February 6, 2016 have a maximum solar insolation of less than 500 W m^{-2} and insolation values measured for only 9-11 hours. In contrast, many late spring and summer days report insolation measured for 14-16 hours per day and reach maximum values above 750 W m^{-2}.

Under conditions with significant available energy for ET, limited available water results in low rates of ET. During water-limited periods, the range of ET rates is small. In contrast, during periods of abundant available water, ET rates have a larger range as the amount of energy available for ET varies. Water-limited conditions, although infrequent, occur primarily in the summer. Under rare drought conditions in the summer of 2016, a minimum soil moisture of 0.009 m^3 m^{-3} was recorded on July 8, 2016, after 13 mm fell in 39 days during a period of high incoming solar radiation. This value is significantly lower than the wilting points reported in the literature (Voyde et al. 2010; DiGiovanni et al. 2013; Starry et al. 2014). With the annual cycling of incoming solar radiation, energy available for ET varies, influencing the available water retention capacity of the substrate and therefore seasonal retention performance. Field capacity on the roof as estimated from the observed soil moisture after runoff has ceased is roughly 0.22 m^3 m^{-3}, but varies spatially across the roof due to localized differences in substrate structure and flow pathways.

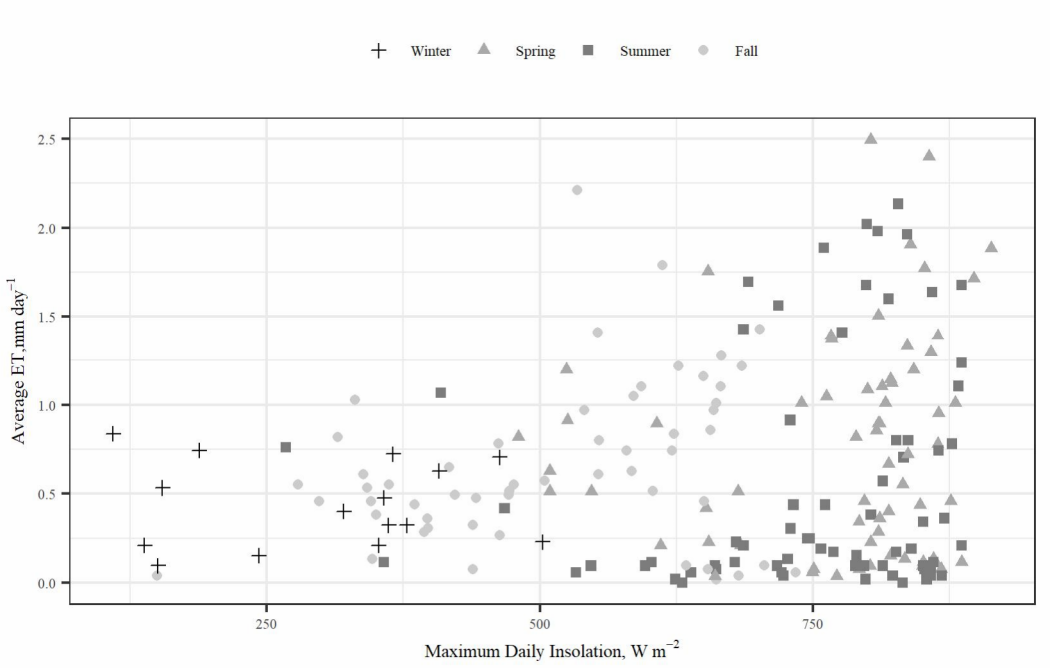

Figure 4.8 *Seasonal trends in average daily evapotranspiration relative to maximum daily insolation on the OnCenter green roof.*

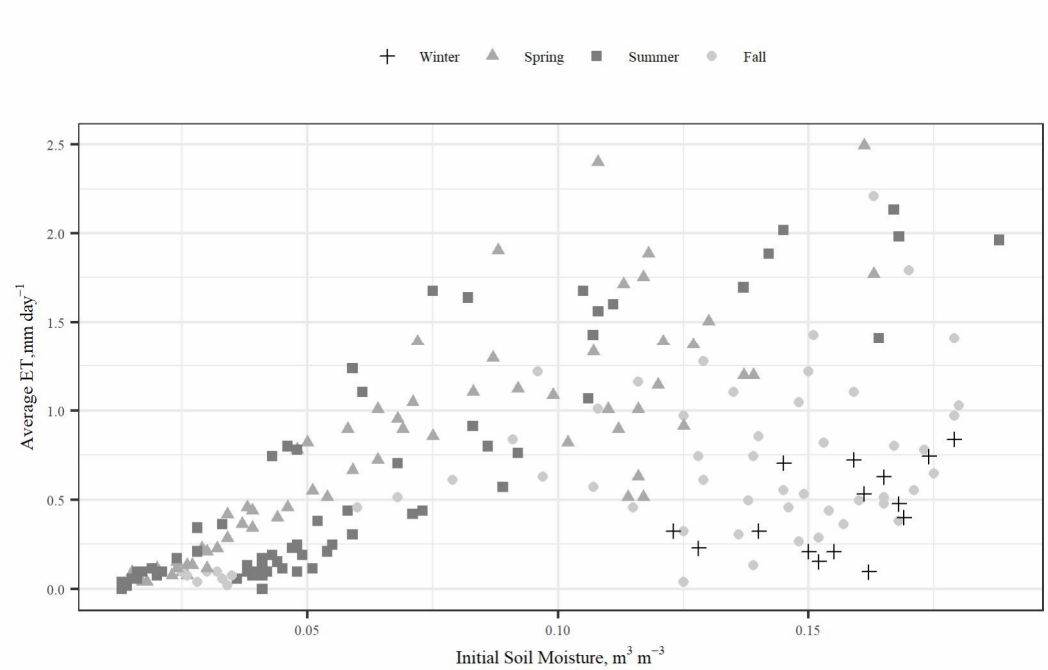

Figure 4.9 *Average daily evapotranspiration relative to daily initial soil moisture on the OnCenter green roof.*

4.5 Conclusions

In this study I examined the rainfall-runoff response of the Onondaga County Convention Center green roof, a large extensive green roof in Syracuse, NY. Dominant hydrologic processes were investigated for their contribution to the overall hydrologic function of the roof. A monitoring program was conducted to measure components of the water mass balance from a 1792 m^2 section of the roof. The roof retained a significant amount of rainfall on an annual basis, but most of that retention occurred during small rainfall events. For large rainfall events, runoff occurred after the retention capacity of the roof was exceeded. The roof was designed to hold a 25.4 mm rain event. Evapotranspiration was found to drive the recovery of the retention capacity between rainfall events. Evapotranspiration can be limited by availability of water at times and by availability of energy at other times; which of these is more important varies with season. Coupled with differences in rainfall characteristics, the variation in evapotranspiration with season is responsible for the difference in performance between winter and summer.

Detention performance metrics, commonly used in the green roof literature, were reported here despite their limitations. Peak delay, the temporal difference between the peak in rainfall and peak in runoff, yields a wide range of values which provided minimal information without additional context. This study further supports the need for care in reporting detention and comparing detention metrics among different roofs. Characteristics of drainage structures on this green roof and on other green roofs can markedly affect detention of stormwater.

This work advances the understanding of extensive green roof performance by considering events across a multi-year study period and in an inland Northeast U.S. climate. This research further supports the need for long-term studies on full-scale green roofs in multiple climates and under natural conditions, as it demonstrates how performance is closely coupled with localized

weather patterns. Future studies should consider green roofs as part of a larger system for managing stormwater in the urban environment.

Chapter 5. Green roofs in our cities: An analysis of two commonly-used modeling methods for the application of green roof technology[3]

5.1 Introduction

Research into stormwater management has considered both the stormwater quality and quantity impact of green roofs and the factors that influence performance both from observational studies and modeling efforts. Studies on green roof hydrologic modeling have a wide range in the literature (Li and Babcock 2014), from simple to complex, though few of these studies consider the models that are frequently used by design professionals and required by regulators. Further, while results from empirical studies suggest variation in regional performance, CN and Cv values in the literature are not widely available (Fassman-Beck et al. 2016).

Design professionals applying these methods rely on local jurisdictions to provide guidance on the appropriate CN and Cv for design, which are often rough estimates based on data from other locations. In larger jurisdictions, where available resources allow the development of guidance documents, justification for parameter selection is not commonly provided. Field studies mentioned above, as well as recommendations of researchers in the field (Fassman-Beck et al. 2016), suggest additional investigation of the curve number and runoff coefficient for the rational method are needed to advance the state of the design practice for green roofs. For this work I aim to further the basis of knowledge available to design professionals, researchers, and regulators by 1) considering methods used to determine green

[3] Squier-Babcock, M. and C. I. Davidson. 2023. "Green roofs in our cities: An analysis of two commonly-used modeling methods for the application of green roof technology." *J. Sustain. Water Built Environ.*, In Review.

roof CN and Cv, 2) quantifying those values for one large extensive green roof in a Northeast U.S. climate, and 3) evaluating the ability of varying CN and Cv values to predict performance for this one roof.

5.2 Methods

Using substrate temperature, snow cover, and snowfall records to eliminate days when the measurements were influenced by snow, the current empirical study measured rainfall and runoff for 727 events during a nearly 7-year study period. Earlier empirical analysis of the OnCenter green roof hydrologic behavior considered 165 events in the first 21-months of this study period, finding a cumulative retention of 56% (Squier-Babcock and Davidson 2020).

5.2.1 Curve Number

The curve number (CN) can convert rainfall to runoff and was developed to quantify the impacts of urban development on runoff hydrology (USDA 1986). Traditionally a CN takes into account soil type and land cover in an area, both measures of infiltration. CNs range from 0 to 100, with a value of 30 for dense vegetation with good infiltration and a value of 98 for a completely impervious area (USDA 1986). The method is used worldwide by design professionals, in part because it was developed and is supported by an agency of the U.S. government, the Natural Resources Conservation Service (NRCS) (Hawkins et al. 2009). Using the curve number, runoff can be estimated for any given rainfall event size:

$$Q = \begin{cases} \dfrac{(P - Ia)^2}{(P - Ia) + S}, P > Ia \\ 0, P < Ia \end{cases} \quad (1)$$

$$S = \frac{25{,}400}{CN} - 254 \quad (2)$$

$$Ia = \lambda * S \quad (3)$$

where S is the potential maximum retention after runoff begins, Ia is the initial abstraction (or initial losses), λ is the initial abstraction coefficient generally assumed as 0.2, P is the rainfall depth, and Q is the estimated runoff (USDA 2004). The equations presented here assume values in millimeters for P, Q, S, and Ia.

Estimation of the curve number is completed using a least squares method which minimizes the cumulative square errors of events for the 313 events for which rainfall exceeded 2 mm. This method is recommended as the most appropriate (Hawkins et al. 2009) and used by other researchers (Carson et al. 2017; Fassman-Beck et al. 2016; Oliveira et al. 2016). Hawkins et al. suggest a bias towards a higher CN when fitting to a data set characterized by low rainfall events. To avoid this problem, the value of CN in this study has also been calculated using the 83 events where rainfall depth exceeds 12.5 mm.

5.2.1.1 Curve Number step function

Growing out of empirical studies which have found green roofs function differently after existing storage capacity is met, another approach to applying a curve number to green roof hydrologic modeling takes the form of a step-function, proposed by Fassman-Beck et al. (2016):

Runoff volume = 0 when:

$$P < S_W \quad (4)$$

$$S_W = D \times PAW \tag{5}$$

$$0 < S_W < 20 - 30\ mm \tag{6}$$

where S_W is the maximum water storage in mm in the growth medium, which represents the volume of water per unit area of roof, D is the growth medium depth in mm and PAW is the plant available water as a fraction. For larger events when precipitation exceeds S_W, runoff volume is calculated using CN = 84. The 20 – 30 mm range is proposed to represent the maximum storage on the roof. In this paper, since the OnCenter green roof was designed to store 25.4 mm of rain, this value is selected as the limit for S_W (Monge 2021).

5.2.1.2 The initial abstraction term

The initial abstraction term is defined as the amount of rainfall held on the roof prior to the onset of runoff. The initial abstraction coefficient λ is commonly defined as 0.20 despite limited source material to justify this value (Hawkins et al. 2009). Researchers have questioned the appropriateness of the initial abstraction relationship presented in Equation (3). Other values for λ have been proposed, and multiple watershed studies have shown $\lambda = 0.05$ to be a more realistic estimate for widespread application (Jiang 2001). However, a change in this term requires a change to CN values reported in standard tables and used by design professionals, and so it is not commonly used by practitioners (Hawkins et al. 2019).

5.2.2 Rational Method and exponential estimation

Originally developed in Ireland, and first applied in the U.S. in 1889 in urban watersheds, the rational method is used to determine the design discharge from a watershed (Dooge 1957; Kuichling 1889; Mulvaney 1851):

$$Q_R = C_V i A \tag{8}$$

where Q_R is the discharge or runoff rate, C_V is a runoff coefficient, i is the design rainfall intensity or average rainfall intensity, and A is the watershed drainage area. Both metric and English units can be employed using this equation, as long as consistent units are used. For the purposes of this work, Q_R has units of $m^3\ s^{-1}$, i has units of $m\ s^{-1}$, and A has units of m^2. The runoff coefficient is the relationship between runoff and rainfall:

$$C_V = \frac{R}{P_R} \tag{9}$$

where R is the total depth of runoff from a watershed, and P_R is the total depth of precipitation. This method is also commonly used worldwide, in particular for the design of storm sewers (Chin 2019; Schärer et al. 2020):

Fassman-Beck et al. (2016) fit C_V values determined from 21 green roofs in varying climates with 289 potential regression models, and found the best fit to take the form:

$$C_V = a * \exp\left(\frac{b}{P_e}\right) \tag{10}$$

where P_e is event precipitation as a depth and a and b are regression coefficients. In this paper, the regression coefficients are fit using the OnCenter data and the model results and compared to models from similar climates.

5.3 Results & Discussion

5.3.1 Data set

The raw data collected at the OnCenter and used in this study expand upon the 21-month dataset investigated by Squier-Babcock and Davidson (2020). From the nearly seven years of data considered here, 727 events remain after the criteria discussed above are applied. Overall, 59.9% of rain which fell in the 727 events is retained. Of these events, 414 are very small events (< 2 mm) accounting for 7.7% of the overall rainfall in the study dataset, while 35 large events (> 20 mm) account for 30% of overall rainfall. Figure 5.1 shows runoff and retention for size categories of events, while details of the 35 large events are given in Table B.1 in Appendix B. Consistent with the results presented in Squier-Babcock and Davidson (2020), most rain falls in large events despite the higher frequency of smaller events. Of the 268 mm of rain that fell as part of very small events, 79.1 % of runoff is retained. In contrast, only 41.1% of runoff from large events is retained. Rain from small and medium storms is retained at percentages between these values, with the overall amount of runoff increasing as event size increases.

With very small events removed (< 2 mm), only 56 rainfall events with a total of 419 mm remain after accounting for winter conditions. A total of 113 events (1018 mm) occur in the spring, 90 events (988 mm) in the summer, and 65 events (824 mm) in fall. Average event retention is lowest in the winter at 39% and highest in the summer at 73%, while spring and fall are 58% and 51% respectively.

5.3.2 Curve number

5.3.2.1 Curve number determined from events

CNs for each of the 313 rainfall-runoff pairs for events where rainfall depth met or exceeded 2 mm ranged from 54 to 100, with a median value of 96 and mean of 95. A least-squares estimate of the 313 events yields CN = 96 as the best fit. CNs are given as integers, so all values used here are rounded to the nearest integer. The CN for each event is compared with the corresponding rainfall and runoff for the event (Figure 5.2). When events with rainfall less than 12.5 mm are removed, a least-squares estimate of the 83 remaining events yields CN = 96.4 as the best fit.

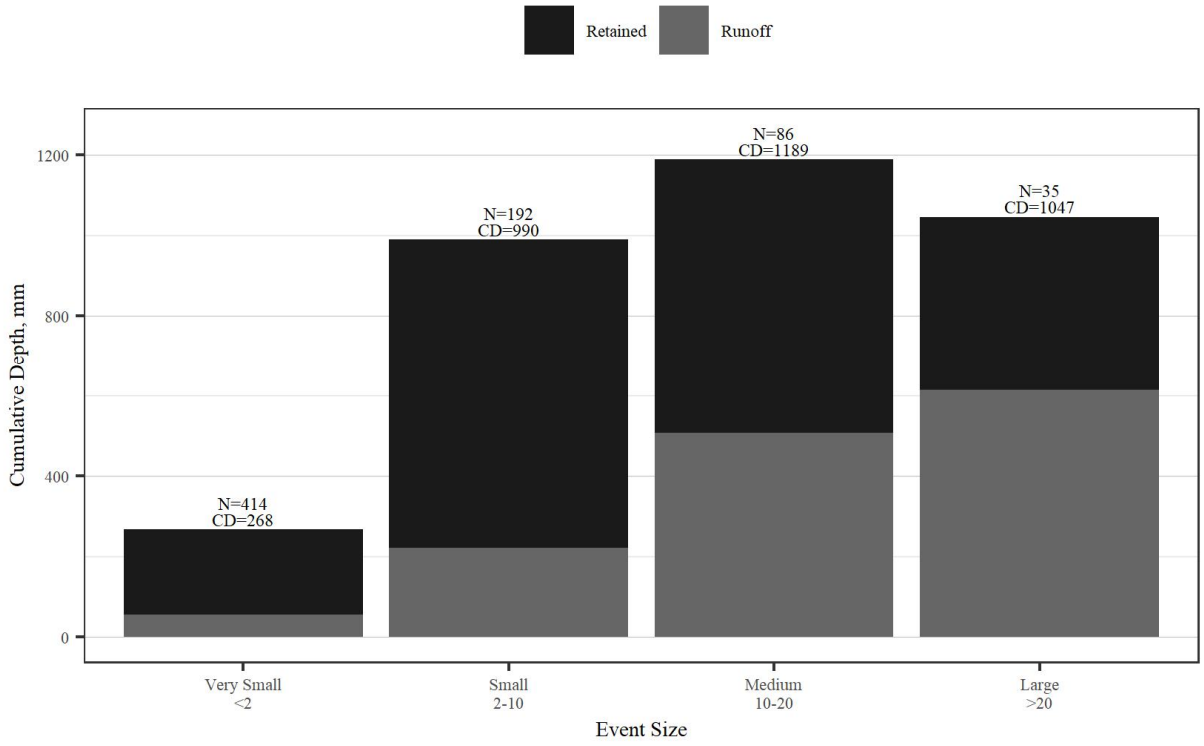

Figure 5.1 *Runoff and retention from the OnCenter green roof, designed to hold a 25.4 mm rainfall event grouped by event size. Cumulative depth (CD) is the sum of runoff and retained depth. Total rainfall over the nearly 7-year study period, excluding snow days, is the sum of cumulative depths in each range – 3495 mm in total.*

The influence of small events to bias the CN towards higher values is well-recognized. However, for the events on this roof, eliminating small events has only a minor influence on the CN. While this result is within the range found on other roofs, the estimated CN could also be skewed as the largest rainfall events in the data set are still not very large. While most events that fall on this roof have a small total depth, most runoff occurs during larger events.

In practice, observed data are not frequently available, and curve numbers for green roofs are assigned by regulators. Design professionals and regulators also look to national guidance and researchers to provide appropriate values. A curve number update included in the draft edition of Chapter 9 of the National Engineering Handbook Part 630 proposes curve numbers by

growth medium depth, adapted from Fassman-Beck et al. (2016); for 7.62 cm of growth medium, a CN of 89 is proposed.

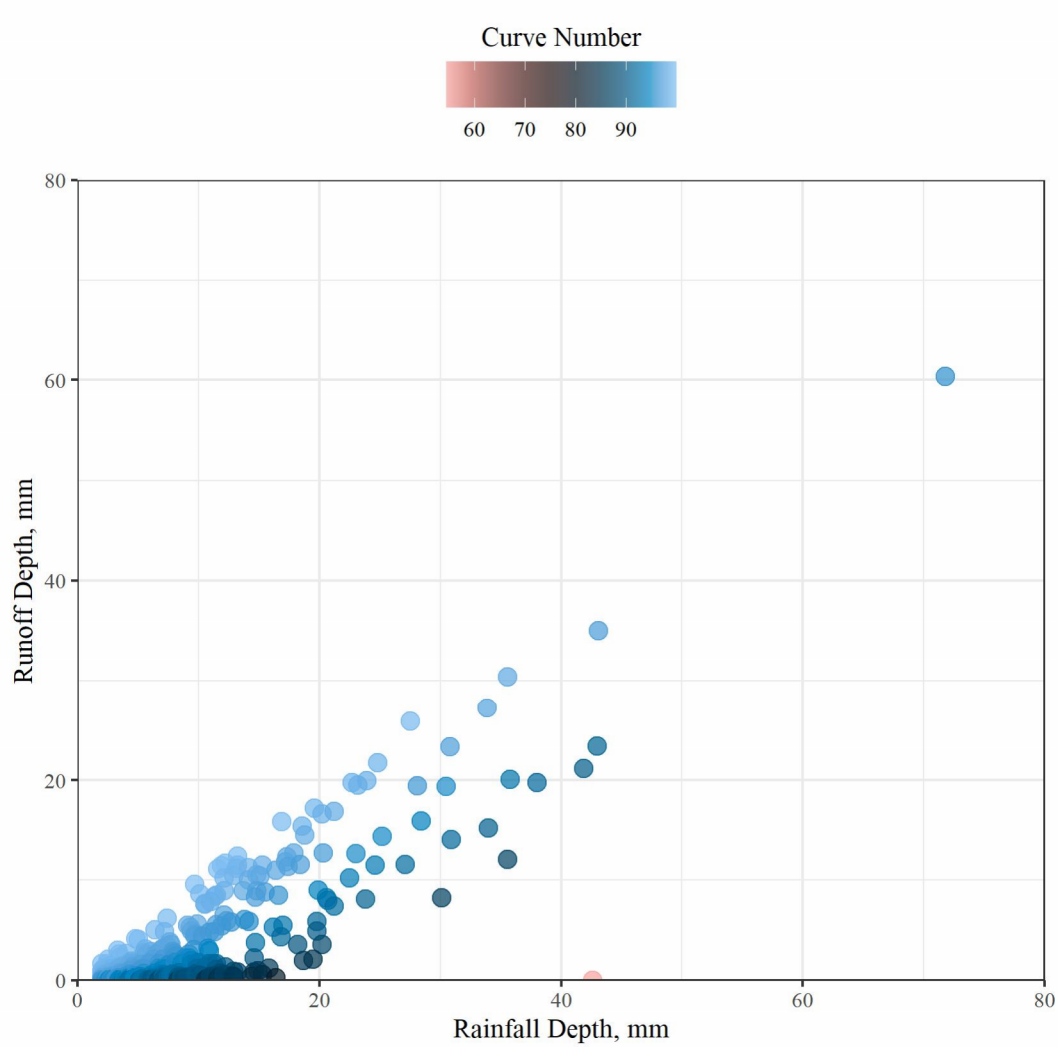

Figure 5.2 *Event curve number in relation to rainfall and runoff depth.*

The 313 observed rainfall-runoff pairs (rainfall depth > 2 mm) are compared with modeled runoff using four curve numbers in Figure B.1. Visually, there is no significant indication that CN = 96 is the best fit. R^2 for CN=96 is only slightly higher than CN = 98. When comparing the slope of their linear models, CN=98 is just slightly closer to 1. The contrast between CN = 96 and 98 versus the lower CN values is clear, and those higher values are a better choice to model runoff from an extensive green roof. Common statistical methods are applied to compare the CN

values, with results shown in Table 1. A wider range of values was tested to confirm the best performance of CN = 96, which has the highest value of NSE. All of the curve numbers evaluated have an NSE greater than zero, meaning they all generally predict runoff better than simply using the mean observed runoff value. R^2 is also highest for CN = 96, but all the CNs considered here provide reasonable fit. In comparing the parameters of the linear models for which R^2 is evaluated, the intercept for CN = 96 approaches zero as the slope approaches 1. Overall, using CN = 96 provides the best estimate of these four curve numbers in determining runoff depth from individual rainfall events on this green roof.

Fassman-Beck et al. (2016) compared rainfall-runoff pairs from 21 green roofs and found a range of CNs from 75 to 96. A narrower range of CNs, between 90 and 96, was found for six of the 21 green roofs included in the study that share a similar climate with the OnCenter roof (Dfb/Dfa). These six roofs were all extensive and ranged in depth between 5 and 14 cm. In Toronto (Dfa), 24 plot-scale green roofs with 10 – 15 cm depth had an average CN of 93 when no irrigation was used (Hill et al. 2017). In New York City, climate zone Cfa, Carson et al. (2017) reported individual event CNs range between 81 and 99 for two extensive green roofs. The CN for the OnCenter fits within this range though skews towards the higher side of the reported values. The OnCenter roof is on the shallower side of the roofs considered in the literature, so it would be expected to store less rainfall within the growth medium prior to the onset of runoff, resulting in a higher CN. Further, the cooler climate in Syracuse relative to cities in the Cfa climate zone likely means less evapotranspiration, the mechanism by which green roofs recover their ability to store rainfall.

Hawkins et al. (2009), in completing a sensitivity analysis of the CN model, found that the runoff results are most sensitive to the selection of CN, even more important than the input of

rainfall. This pattern suggests the selection of the best fit CN for a given green roof is important to design. The differences between four selected CNs for the 1, 10, and 100-yr 24-hr Syracuse area design storms are shown in Figure 5.3. The large differences between the runoff values, even within the relatively narrow range of proposed CNs, show how easily poor CN selection could result in inaccurate green roof performance predictions, especially for large events.

Table 5.1 *Goodness of fit criteria NSE and R^2 for model assessment of four curve numbers.*

	Curve Number			
	84	89	96	98
NSE	0.243	0.495	0.707	0.519
R^2	0.534	0.674	0.738	0.734
Intercept	-0.016	-0.339	0.692	2.00
Slope	0.302	0.497	0.887	1.03

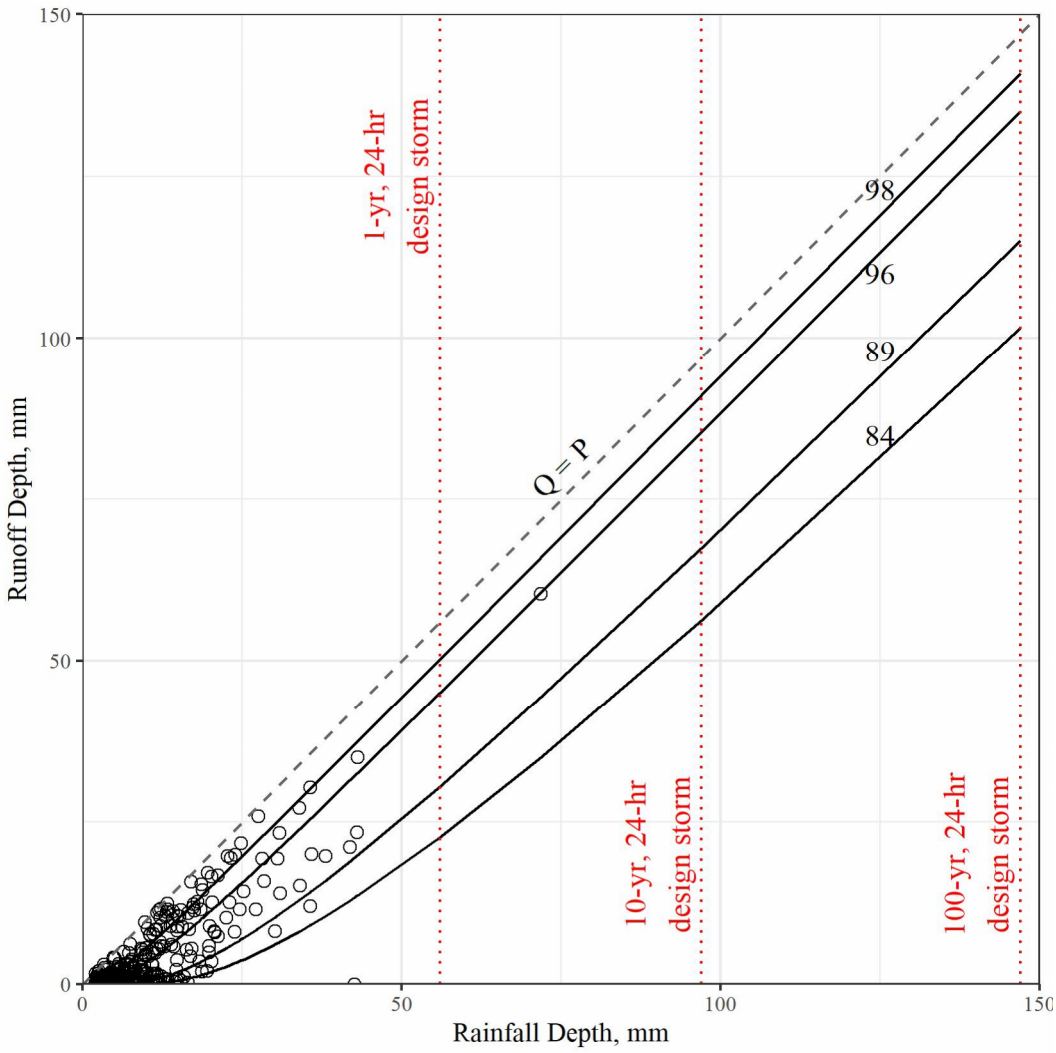

Figure 5.3 *Observed rainfall-runoff pairs and modeled runoff for four curve numbers. Modeled runoff uses the observed rainfall and three design storm rainfall depths as inputs.*

5.3.2.2 Evaluate curve number using step number function

Adapting the CN method, Fassman-Beck et al. (2016) propose adding a step function to improve the predictive power of the method within the design framework used by design professionals and required in many jurisdictions. The proposed step-function method is applied using 25.4 mm as the storage capacity for the OnCenter roof, per the roof's design (Monge 2021). A value that is determined from the roof design is appropriate here as this is what would

be available to design professionals. The suggested CN of 84 for events where P > Sw is compared with other CNs. For each CN, modeled and observed runoff are fit to a linear regression (not shown). The R^2 values are all a good fit. Studies have shown that after the green roof storage capacity is met, any additional rainfall becomes runoff (Vesuviano et al. 2013; Carter and Rasmussen 2006; Voyde et al. 2010; Stovin et al. 2012), consistent with the results here that CN = 98 is the best fit after storage is met.

5.3.2.3 Calibrate curve number with changing lambda

Using $\lambda = 0.05$ with CN = 96 slightly worsens the modeled runoff fit for events larger than 2 mm. Per Hawkins et al. (2019) the use of a different lambda requires recalibration of the CN values. The least squares estimate is applied to $\lambda = 0.05$ which yields CN = 98. Parameters for the fit using $\lambda = 0.05$ are given in Table 2 below. Parameters for the $\lambda = 0.20$ were given above in Table 1. While the slopes for both CNs are close to 1, the intercept for CN = 96 is much smaller than CN = 98. Overall, CN = 96 with $\lambda = 0.20$ is a better fit for the data presented here.

Table 5.2 *Efficiency criteria for two curve numbers and lambda = 0.05*

	Curve Number	
	96	98
NSE	0.664	0.443
R^2	0.738	0.733
Intercept	1.43	2.53
Slope	0.924	1.04

5.3.2.4 Performance of other CN values

Given the variability in reported CN even within the same climate, and the significant variation in green roof design, it is likely that many green roofs are modeled using an inappropriate CN. For the OnCenter green roof, NSE increases roughly linearly from 0.034 to 0.707 as CN increases from 79 to 96. As CN increases past 96 however, NSE drops to 0.519 at CN = 98. Acceptable model performance varies with the best values of NSE approaching 1.

It is also of interest to express the difference in performance in terms of volume of stormwater. The difference for the 1-year, 24-hour design storm (56 mm) between CN = 84 and CN = 95 is 20 mm according to Figure 5.3, a small depth, but this corresponds to a large runoff value for the OnCenter roof, namely 111 m^3. For the 100-year, 24-hour event (147 mm) this value increases to a 30.5 mm difference, or 169 m^3. The impact of this potential underestimate on urban hydrology is magnified by considering that in larger cities this roof may be one of many. An overestimate, in contrast, would provide additional storage for cities, but at a significantly increased cost.

5.3.2.5 Seasonal comparison of CN estimate

To further investigate the variation of CN at the OnCenter green roof, the data are grouped by meteorological season (Winter: Dec-Feb; Spring: Mar-May, etc.) and least squares regression is used to determine CN. The lowest CN is determined for the summer at CN = 95, while the highest is found in the winter, CN = 99. Spring (CN=96) is nearest to the predicted annual values, while fall is slightly higher (CN=97). Higher values are found in the winter when retention is lower. Lower retention occurs when the storage capacity of the roof does not recover between events. Lower evapotranspiration during the winter renders the green roof similar to an impervious surface when using this simplified model. When evapotranspiration rates are higher during the summer months, more retention occurs and the estimated CN is lower. The analysis here does not consider snowmelt or the influence of snowmelt on future retention. In Syracuse, snow occurs regularly between October and April, influencing fall, winter, and spring values determined here. The lowest CN, found in the summer, occurs as evapotranspiration rates are at their highest, allowing the storage capacity to regenerate between events. While the small difference between these integer values may seem unimportant, each increase in CN by a value

of 1 is equivalent to roughly 2.5 mm of runoff depth from the 1-year, 24-hr design storm in Syracuse, accounting for an increase of 14 m^3 for the OnCenter green roof.

5.3.3 Rational Method

5.3.3.1 Determine Cv from rainfall-runoff pairs

From Eq. 9, Cv is determined for each rainfall-runoff pair and ranges between 0 and 0.99 with a median of 0.22 and mean of 0.31. This value ranges from a typical value for lawns (0.05 – 0.10) to slightly higher and is much smaller than the typical value used for impervious roofs (0.75 – 0.95) (McCuen 2005). Cv is a ratio between runoff depth and rainfall depth, and the large number of events with small runoff depth skew the data towards a smaller value. When medium and large events are considered (Rainfall Depth > 10 mm), resulting Cv's are much higher, with a mean of 0.46 and a median of 0.46. Comparing Cv to rainfall depth there is no observable pattern . Hill et al. (2017) found Cv = 0.4 in a study in Toronto with 24 small green roof plots of 10 and 15 cm depth using rainfall events from two seasons between May and October. Schärer et al. (2020) measured rainfall at 4 plot scale green roofs at different sites across Norway (climate Cfb and Dfb) and found Cv ranged from 0.023 to 0.41. In Brazil, Loiola (2019) considered runoff from a 5 cm deep substrate on green roof plots with initial substrate in both wet and dry conditions and found mean Cv values of 0.66 and 0.27, respectively. While runoff coefficient values for landcover are provided in standard tables, those for newer practices are generally provided by the agency with jurisdiction. In Philadelphia, for example, the design runoff coefficient for a green roof is 0.40 (Philadelphia Water Department, 2020), while New York City code specifies a Cv of 0.70 for a design for any runoff event over four inches in depth (NYC Administrative Code 2021).

Antecedent soil moisture is inversely proportional to the available storage within the growth medium (Squier-Babcock and Davidson 2020; Beretta et al. 2014; Stovin et al. 2012). However, in this dataset there is no apparent relationship between Cv and initial soil moisture (not shown). By looking at an individual event (Cv = 89), the relationship between soil moisture, runoff and rainfall depth is seen (Figure 5.4). A large event following a dry period is chosen for this comparison. The event shown in Figure 5.4 has total rainfall 71.8 mm and total runoff of 66.8 mm, with an initial soil moisture of 0.04 m^3 m^{-3}. Despite the low initial soil moisture, the event is large enough that the retention capacity of the roof is met. For context, this event falls between the 2-year and 5-year design storm for Syracuse, NY. When determining Cv from event data for use in design, it is important to consider the available storage relative to the size of the design events. The mean and median event values calculated here are too low for most design storms for extensive green roofs. A more conservative Cv selection for design storms would be between 0.65 and 0.85, the range of values when available storage is small (initial soil moisture is high). One governing limit available to practitioners, to determine the appropriate range of Cv values, would be the ratio between design maximum water capacity and design storm size. When this ratio exceeds 1, the use of a lower Cv may be justified. Another way to approach this would be to limit the use of the rational method for green roofs with a shallower depth and therefore a lower maximum water capacity, similar to the approach taken in the New York City design manual (NYC Environmental Protection 2018). This work at the OnCenter supports the use of

regional Cv values as well, as precipitation patterns that determine design storm size and inter-event recovery of available water storage are products of regional climate.

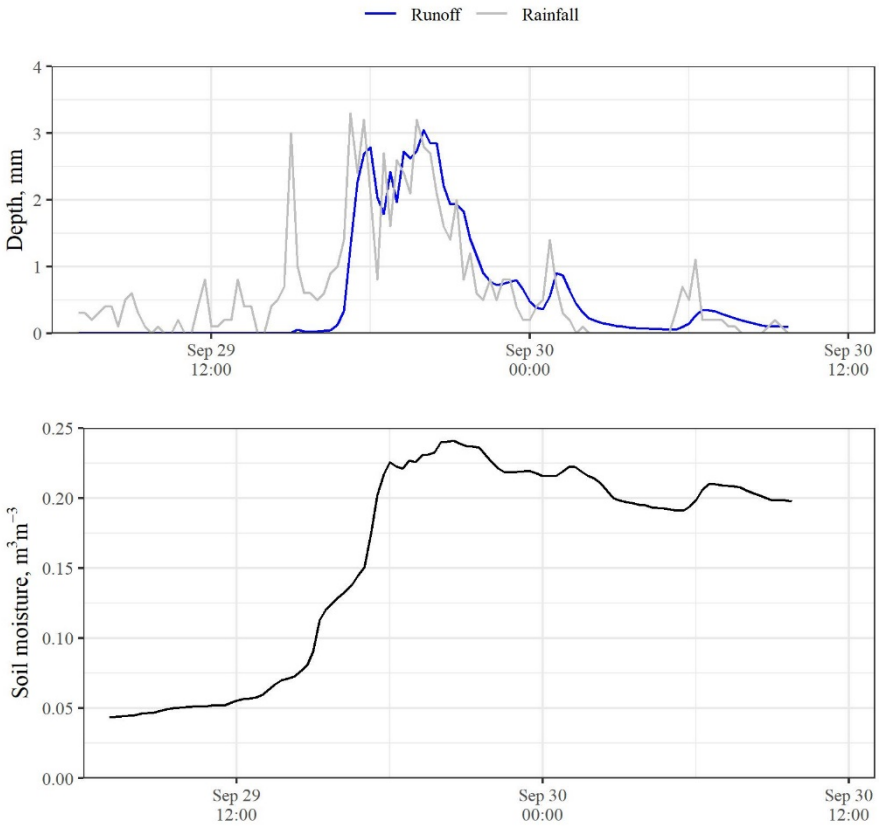

Figure 5.4 *One large rain event (Total depth = 71.8 mm) on the OnCenter green roof that started with a relatively low soil moisture (0.04 m^3m^{-3}) and for which the maximum water capacity was quickly exceeded. The individual runoff coefficient estimated for this event was high at 0.89.*

5.3.3.2 Regional exponential model for Cv

Previous work completed by Fassman-Beck et al. (2016) identified a nonlinear model for estimating Cv using data sets from multiple green roofs in different climates (Equation 10). Extending this work to the Dfb climate zone, using the OnCenter green roof, a nonlinear parameter estimation shows a = 0.574 and b = -4.15. Parameters for extensive green roofs in two

adjacent climate zones, developed by Fassman-Beck et al., are applied using the OnCenter rainfall as input, given in Figure 5.5. The Dfb/Cfa4 model initially follows a similar shape to that of the OnCenter's Dfb model, however it continues climbing and levels off at a higher value (Cv = 0.82). The Dfb model climbs quickly and then rapidly levels off reaching Cv = 0.54 for the largest events. The model for the Dfa5 climate zone has a similar shape but increases at a lower rate. However, it reaches a maximum value of 0.60 as rainfall depth increases, higher than the Dfb model. Substrate depth for the roofs included by Fassman-Beck et al. in the development of the Dfb/Cfa and Dfa models relative to the OnCenter roof depth may also explain in part the difference in the curves in Figure 5.5. The Dfb/Cfa model roof has 140 mm of growth medium, roughly double that of the OnCenter (76.2 mm), while the five roofs included in the Dfa model have an average depth of 111 mm. The larger available water capacity on the roofs with greater depth explains the more gradual approach and lower maximum Cv values. However, there is some variability in the maximum values reached in this plot, which is not fully explained by roof depth. This variability could be a result of the limited number of events used to develop the original models (only 8 for the Dfb/Cfa model). The variability could also be an artifact of the limited number of large events in the OnCenter dataset, and likely a larger runoff coefficient

[4] One study site in Pittsburgh, PA was used to develop the model for the Dfb/Cfa climate zone (Fassman-Beck et al. 2016).

[5] Four study sites in Michigan, Illinois, and Pennsylvania were used to develop the model for the Dfa climate zone. A study site in Toronto, Canada was also considered but did not satisfy the constraints (Fassman-Beck et al. 2016).

would be more appropriate for storm events which exceed the storage threshold of a green roof, as argued in the previous section.

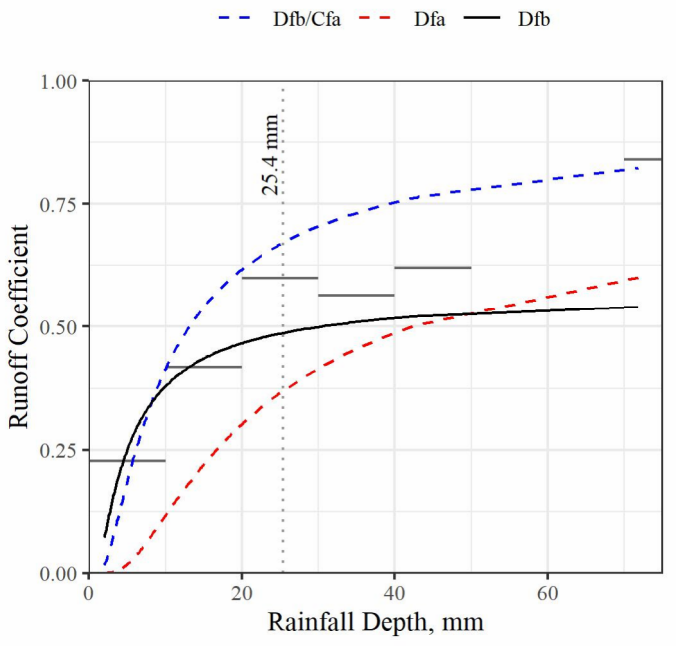

Figure 5.5 *Comparison of estimated volumetric runoff coefficients and three exponential models fit for different climate zones. Parameters for Dfb/Cfa and Dfa are taken from Fassman-Beck et al. (2016). Parameters for the Dfb climate zone are fit from data measured at the OnCenter in Syracuse, NY. Rainfall measured on the OnCenter is used as input for each model. Runoff coefficients are averaged for each 10 mm range of precipitation and represented by horizontal lines. No rainfall fell in the 50-60 mm or 60-70 mm ranges and only one event is included for the 70-80 mm range (partially off the plot). A dotted vertical line indicates the rainfall depth the green roof was designed to retain, 25.4 mm (Monge 2021).*

5.3.4 OnCenter green roof and local regulations

While the OnCenter green roof was a retrofit and therefore not subject to permit requirements for stormwater discharges during construction[6], it is nevertheless a useful tool for the comparison of the regulations practitioners must comply with. The methods previously

[6] Note that the OnCenter green roof was part of a larger initiative in the Onondaga Lake Watershed to capture and treat runoff. This initiative was part of an amended consent judgment related to previous violations of the Clean Water Act and was branded SaveTheRain. Under this initiative the OnCenter green roof was designed to capture a 1" depth of rainfall, or approximately 1 million gallons annually (Monge 2021).

discussed in this paper, CN and rational method, are generally accepted methods for showing compliance with these regulations. The applicable requirements for development in the City of Syracuse depend on the sewer connection – separate or combined. The OnCenter falls within a combined sewershed and would therefore be regulated by the City of Syracuse if ground disturbance had exceeded 929 m^2. Had the OnCenter been newly constructed, instead of retrofit with the green roof, designers would have been required to limit discharge from the roof to 0.019 $m^3\ s^{-1}$ for the 10-yr, 30-min design event, 3.3 cm in Syracuse[7]. A design discharge limit, such as that required by the City of Syracuse, is not dissimilar to that used in other combined sewer communities, including New York City (NYC Environmental Protection 2020). To compare the rational and CN methods, the peak discharge from the design event is calculated using Cv = 0.75 and CN = 96. A Cv of 0.75 is selected from the middle of the estimated conservative range. The rational method yields a peak discharge of 0.076 $m^3\ s^{-1}$ and the CN method yields a peak discharge of 0.106 $m^3\ s^{-1}$. For comparison, an impervious roof would have a Cv = 0.95 and CN = 98, with peak flows of 0.097 $m^3\ s^{-1}$ and 0.133 $m^3\ s^{-1}$, respectively. CN peak discharge is calculated using HydroCAD v10.10-5a with a time of concentration of 15 minutes, the estimated hydrologically longest path across the roof. Using the higher peak flow, the CN method peak discharge, and the modeling software, a 91 m^3 detention tank with a 7.62 cm outlet orifice would be needed in addition to the green roof to comply with the City's requirements. Without the green roof, the size of the detention tank increases to 127 m^3, even assuming no decrease in time of concentration. It should be noted that this comparison only considers the green roof and

[7] Regulations are given in English units by the City of Syracuse: a 10,000 sq. ft. disturbance limit, the 10-yr, 30-min design event is 1.3 inches, and a discharge limit of 0.5 CFS per acre of disturbance.

ignores the impact of other impervious area that would be included if the building were new construction, such as sidewalks and loading docks. In practice, these areas would be included in the design to comply with requirements.

5.4 Conclusions

The curve number and the rational method are applied differently in practice. The rational method only predicts peak flow whereas the CN provides a total storm volume, or when combined with other methods such as TR-55 and TR-20, a full runoff hydrograph. Despite these differences, both methods play a role in stormwater design and are commonly used across the globe. There are some similarities in the results of both models here relative to the literature. For the OnCenter green roof, the best-fit CN and Cv are higher than those found in the literature, suggesting slightly greater runoff values compared with green roofs with greater depth of growth medium. To some extent this is the result of coupled retention and detention processes on the roof. Variations in the values of CN and Cv presented in the literature are likely due to variation in green roof systems and local weather. For example, higher event retention can be expected in areas with higher rates of evapotranspiration or during seasons of higher evapotranspiration. A greater depth of a green roof and the presence of a drainage or reservoir layer may also increase the retention capacity. Such an increase may result in a CN or Cv value closer to those seen in natural settings.

Regulators and practitioners look to researchers to establish appropriate values which allow the incorporation of emerging technologies into an existing system. Regardless of whether the curve number and the rational method are appropriate tools for stormwater management, these methods remain the accepted state of the practice for much of the world. Thus, the importance of continuing green roof studies over many years to capture larger events is crucial to

quantifying the contribution green roofs can make to managing urban stormwater. At the same time, the use of recurrence intervals for storms of various sizes is likely to become less reliable due to changing climate.

Overall, green roofs are one important tool available to the modern practitioner to manage stormwater. Future work should consider the application of green roofs in conjunction with other green and gray infrastructure to meet design goals. Regulatory agencies should consider green roofs within the context of the overall urban environment. Research performed at various scales, from one city block to multiple sewersheds, can identify areas where green roofs would be most beneficial. Current regulations, and this research, do not consider the additional ecosystem services provided by a green roof in a quantifiable way. Future regulation and design guidance should provide a mechanism to account for these benefits, while maintaining the stormwater management design goals.

Chapter 6. Conclusions

6.1 Summary

The overall intent of this research is to advance our collective knowledge of the role green roofs can play in improving the resilience of our cities to extreme events caused by climate change. While green roofs are increasingly adopted in cities across the globe, their actual performance has not been adequately quantified. In this work I aim to fill part of that gap by conducting measurements to quantify thermal and hydrologic performance of an extensive green roof in Syracuse, NY and by considering the appropriateness of the modern design engineer's efforts to model green roofs. In this summary I review the overall findings of the current work in relation to the goals stated earlier and present the contributions of this work. This is followed by a discussion of the limitations of the work and recommendations for future research.

6.2 Thermal Findings

A monitoring campaign was undertaken to better understand the thermal performance of the green roof in different seasons of the year. The growth medium and vegetation can contribute to reduction in heat transfer across the building envelope, but the thermal resistance provided by the insulation layer limits the contribution of the green roof. During summer months total daily solar input is highest and drives downward (negative) heat fluxes through the roof. During other times of the year, the heat flux through the roof is generally upward (positive). In the winter months, an accumulated snowpack behaves as an insulating layer on the roof, thermally isolating the green roof from ambient weather. During this period, the heat flux through all layers of the green roof and the roof structure reaches a quasi-steady state so that material thermal properties can be measured. These material properties generally agree with those reported in the literature and by manufacturers, except for an area where it appears that a grounding screen allowed for trapped

air. These results demonstrate the importance of measuring and reporting material properties for all layers of the roof when the entire roof is considered.

6.3 Hydrologic Findings

In this study, I also examined the rainfall-runoff response of the green roof during several years of varying rainfall. A monitoring program was conducted to measure components of the water mass balance from specified areas of the roof. The roof retained a significant amount of rainfall on an annual basis, but most of that retention occurred during small rainfall events. For large rainfall events, runoff occurred after the retention capacity of the roof was exceeded. The roof was designed to hold a 25.4 mm rain event. Evapotranspiration was found to drive the recovery of the retention capacity between rainfall events. Evapotranspiration can be limited by availability of water at times and by availability of energy at other times; which of these is more important varies with season. Coupled with differences in rainfall characteristics, the variation in evapotranspiration with season is responsible for the difference in performance between winter and summer.

Detention performance metrics, commonly used in the green roof literature, were reported here despite their limitations. Peak delay, the temporal difference between the peak in rainfall and peak in runoff, yields a wide range of values which provided minimal information without additional context. This study further supports the need for care in reporting detention and comparing detention metrics among different roofs. Characteristics of drainage structures on this green roof and on other green roofs can markedly affect detention of stormwater.

This work advances the understanding of extensive green roof performance by considering events across a study period in an inland Northeast U.S. climate. The research further supports

the need for long-term studies on full-scale green roofs in multiple climates and under natural conditions, as it demonstrates how performance is closely coupled with localized weather patterns.

6.4 Modeling Findings

The curve number and the rational method are applied differently in practice. The rational method only predicts peak flow whereas the CN provides a total storm volume, or when combined with other methods such as TR-55 and TR-20, a full runoff hydrograph. Despite these differences, both methods play a role in stormwater design and are commonly used across the globe. There are some similarities in the results of both models here relative to the literature. For the OnCenter green roof, the best-fit CN and Cv are higher than those found in the literature, suggesting slightly greater runoff values compared to green roofs with greater depth of growth medium. To some extent this pattern is the result of coupled retention and detention processes on the roof. Variations in the values of CN and Cv presented in the literature are likely due to variation in green roof systems and local weather. For example, higher event retention can be expected in areas with higher rates of evapotranspiration or during times of higher evapotranspiration. A greater depth of a green roof and the presence of a drainage or reservoir layer may also increase the retention capacity. Such an increase may result in a CN or Cv value closer to those seen in natural settings.

Regulators and practitioners look to researchers to establish appropriate values which allow the incorporation of emerging technologies into an existing system. Regardless of whether the curve number and the rational method are appropriate tools for stormwater management, these methods remain the accepted state of the practice for much of the world. Thus, the importance of continuing green roof studies over many years to capture larger events is crucial to quantifying

the contribution green roofs can make to managing urban stormwater. At the same time, the use of recurrence intervals for storms of various sizes is likely to become less reliable due to changing climate.

6.5 Contributions

Overall, this work quantified the thermal and hydrologic performance of an extensive green roof in Syracuse, NY. At a basic level, this study included the design and establishment of an extensive green roof monitoring system, used both in this work and in the work of other researchers, producing multiple publications in addition to those generated by this research. Further, this monitoring system remains operational and the data collected are available for use by future researchers.

In quantifying the thermal performance of the green roof, a series of R-values for green roof materials were generated. Both the methodology and these properties are of use to future researchers and those developing green roof materials.

In quantifying the hydrologic performance of the green roof, the performance of one green roof under specific climate conditions is added to the growing body of literature, allowing researchers, design professionals, and regulators to better understand the potential contributions of this technology to their systems.

By expanding the analysis to consider common modeling methods, additional data points are added to the limited data set identifying the appropriate values for use in these models. Regulators and design professionals can use this information to carefully consider the application of the models and the appropriate parameters in real-world applications.

6.6 Limitations and Future Work

The unique climate in Syracuse frequently leads to consistent snow cover for much, if not all, of the heating season. This feature of the climate limited the ability to quantify the contribution of the green roof to heat loss during the coldest months. Future studies should consider the impact of green roofs to insulate a building in both cooling and heating seasons, especially during winter at locations where there is much less snow than in Syracuse. The simple methodology presented here could be applied to green roof plots where the ambient environment could be controlled to measure the thermal properties of different green roof materials.

Analysis of hydrologic performance of the green roof was limited initially to three and then to nearly seven years of data. Despite this, the largest event captured fell between a 2- and 5-year, 24-hour design event for the region. Design practitioners frequently use the 1-, 10-, and 100-year design events, as generally required by regulators when designing stormwater management systems, including green roofs. Future work should continue to collect data over longer periods of time, with the aim of quantifying green roof performance during larger rainstorms. This work could then be used to inform both design practitioners and regulators in the appropriateness of green roofs for stormwater management under different conditions.

Green roofs do not exist in a vacuum, yet most research, including this study, quantifies their hydrologic performance without consideration for the systems they operate in. Future work should consider both the application of green roofs in conjunction with other green and gray infrastructure, and the contribution of green roofs relative to their placement and function within a sewershed.

One approach would be to consider the integration of multiple green infrastructure technologies or of using both green and gray infrastructure together. Green roofs have limited storage capacity; however, this capacity is restored via evapotranspiration during dry weather. Therefore, the opportunity exists to use detention technologies in tandem with green roofs to provide increased stormwater management performance. The need also exists to consider the impact of green roofs on overall sewer system flows, specifically in communities with combined sewer systems and urban flooding. Optimizing the placement of green roofs and the specific need of a localized area with a sewershed can allow for improved design of green roofs on a per-site basis.

Important to the success of green roofs are the models used by practitioners when designing green roofs and the accepted parameters set by regulators. The research presented here considers only the CN and Cv values from one extensive green roof. Variation in both climate and green roof design will impact these values. Future work should expand upon the efforts here to quantify appropriate CN and Cv values across a wider range of green roof designs and climates. One approach could be to develop relationships between green roof design parameters and variations in these values. Further, continued development of models to predict these appropriate terms is key to accurate modeling of green roofs, as they are set within the larger context of existing stormwater management systems and programs.

In this study I did not consider the contribution of any of the other ecosystem services reported in the literature, including impacts on the microclimate or habitat. A methodology to quantify these ecosystem services and provide credit requires a shift in regulatory thinking but is necessary when cheaper solutions exist to provide the same thermal and stormwater management benefits. Future work should consider the cumulative impact of these benefits and provide a

regulatory framework to quantify their contribution and continue to encourage adoption of the technology where appropriate.

Appendix A

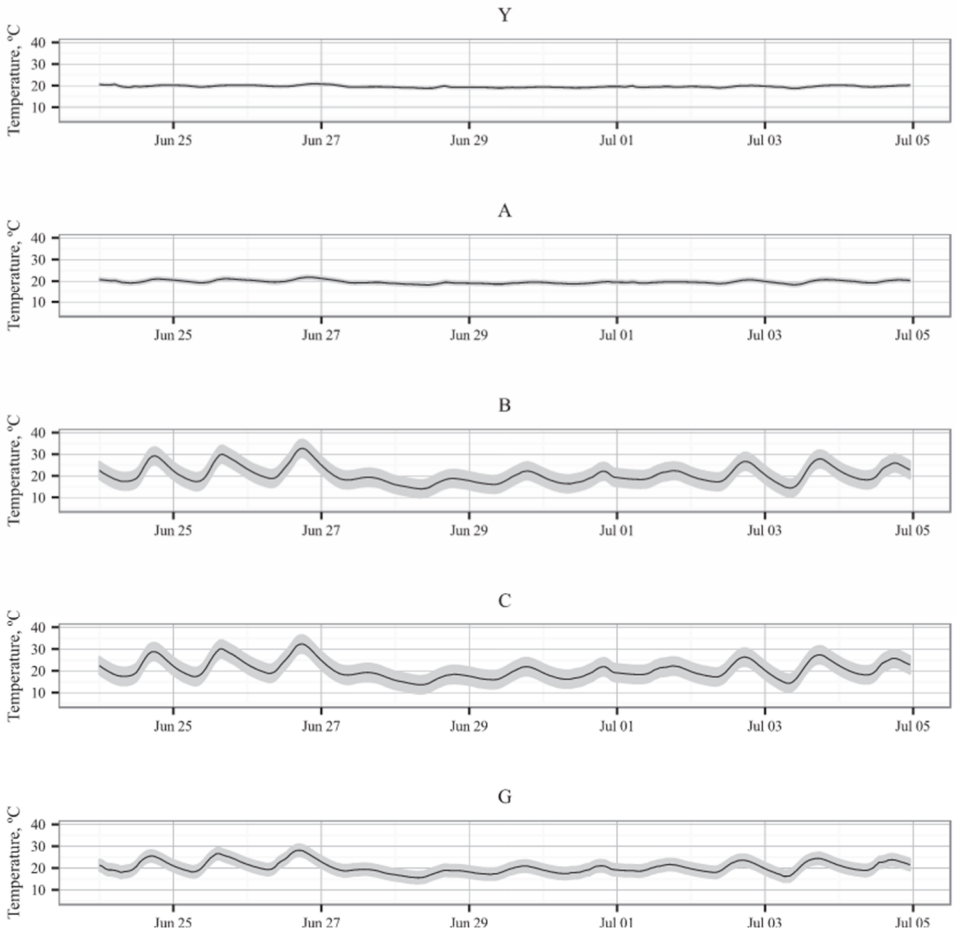

Figure A.1 *Temperature and standard deviation for 5 layers of the OnCenter green roof measured during 11 days in June 2015 characteristic of summer in Syracuse, NY.*

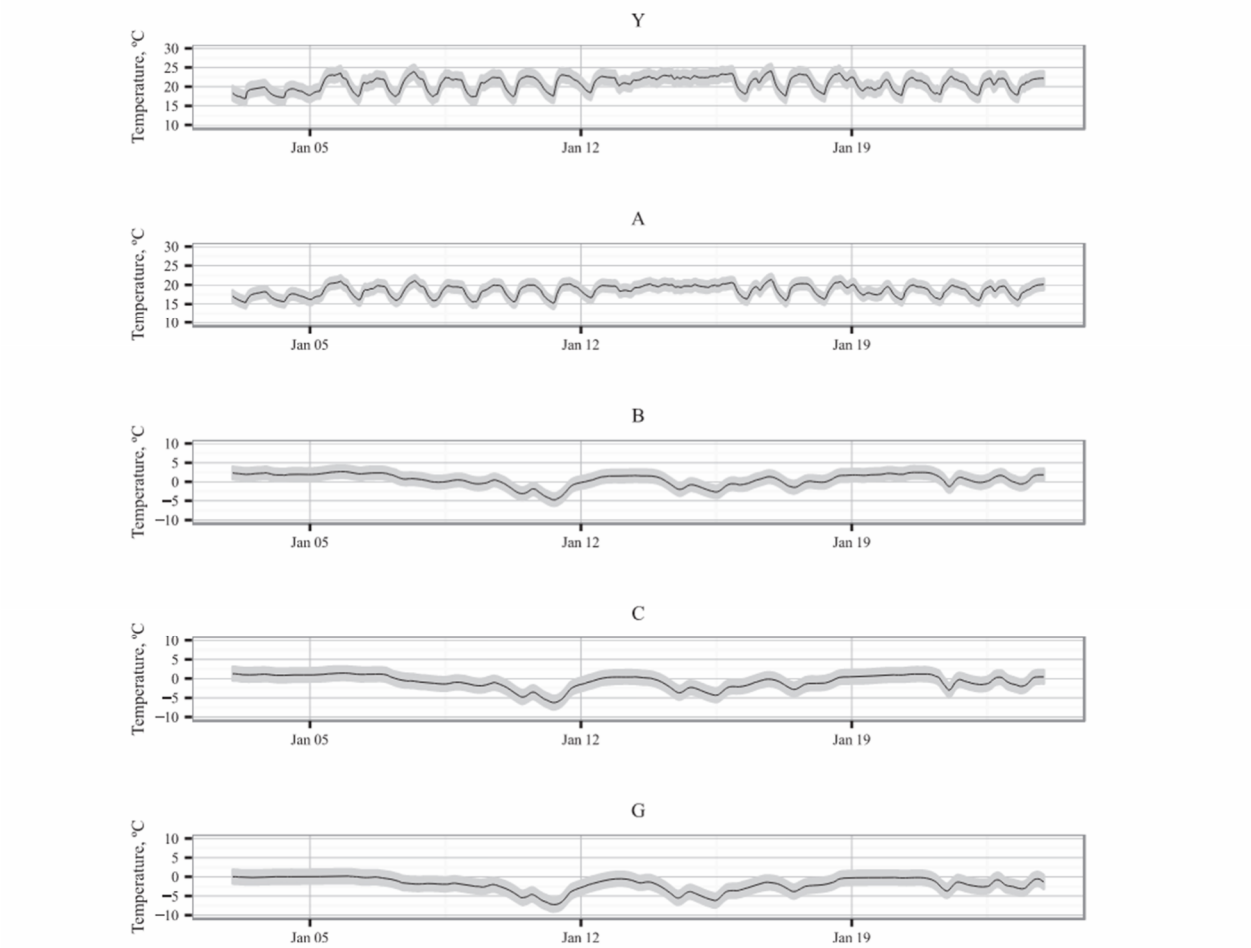

Figure A.2 *Temperature and standard deviation for 5 layers of the OnCenter green roof measured during 19 days in January 2015 representative of winter in Syracuse, NY.*

Appendix B

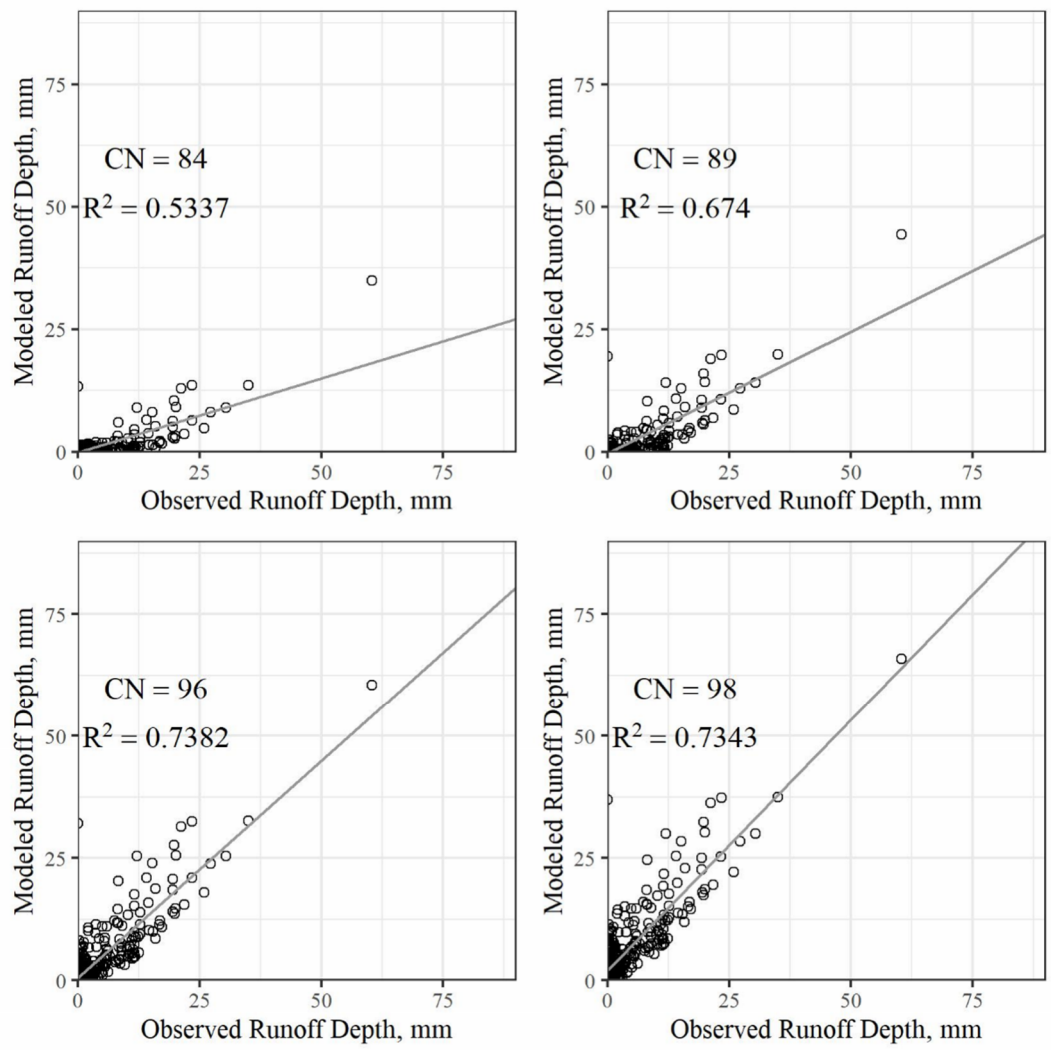

Figure B.1 *313 observed rainfall-runoff pairs (rainfall depth > 2 mm) are compared with modeled runoff using four curve numbers.*

Table B.1 *Details for 35 events which exceed 20 mm in total depth. Retention depth is calculated as the difference between rainfall and runoff depth. Initial soil moisture is the average of the four sensors for the timestep preceding the onset of rain. Initial soil moisture is not available for two events due to equipment failure.*

Start Date	Rainfall Depth, mm	Retention Depth, mm	Initial soil moisture, $m^3\ m^{-3}$
October 15, 2014	35.6	5.21	0.084
May 18, 2015	34	18.8	0.038
May 30, 2015	41.9	20.8	0.019
June 14, 2015	20.3	7.62	--
June 27, 2015	43.0	19.6	--
June 30, 2015	58.3	0.251	0.148
September 29, 2015	71.8	11.4	0.040
October 9, 2015	23.0	10.3	0.075
May 29, 2016	30.1	21.8	0.017
September 8, 2016	20.2	15.6	0.047
September 17, 2016	30.9	16.8	0.036
September 18, 2016	23.2	3.18	0.146
November 2, 2016	23.9	3.94	0.165
March 30, 2017	27.5	1.61	0.138
April 3, 2017	24.8	3.07	0.138
April 20, 2017	20.2	3.61	0.127
May 1, 2017	20.6	11.5	0.085
May 4, 2017	22.7	2.95	0.125
June 30, 2017	25.2	10.8	0.108
May 13, 2019	33.9	6.65	0.193
June 5, 2019	24.6	13.1	0.097
June 19, 2019	22.5	12.3	0.090
July 16, 2019	35.6	23.6	0.012
August 28, 2019	20.7	12.7	0.053
September 1, 2019	21.2	13.8	0.097
October 6, 2019	30.8	7.43	0.109
October 16, 2019	28.4	12.5	0.074
October 30, 2019	43.1	8.10	0.113

Start Date	Rainfall Depth, mm	Retention Depth, mm	Initial soil moisture, $m^3\ m^{-3}$
December 29, 2019	21.2	4.35	0.132
April 30, 2020	28.1	8.68	0.109
July 11, 2020	30.5	11.1	0.062
July 16, 2020	38	18.2	0.064
August 4, 2020	23.8	15.7	0.047
August 27, 2020	35.8	15.7	0.029
September 29, 2020	27.1	15.6	0.027

References

Abualfaraj, N., et al. 2018. “Monitoring and modeling the long-term rainfall-runoff response of the Jacob K. Javits center green roof.” *Water-SUI*, 10, 1–23. https://doi:10.3390/w10111494.

Alexandri, E. and P. Jones. 2007. “Developing a one-dimensional heat and mass transfer algorithm for describing the effect of green roofs on the built environment: Comparison with experimental results.” *Build Environ*, 42, 2835-2849. https://doi:10.1016/j.buildenv.2006.07.004.

Andrews, F. and J. Guillaume. 2016. Hydromad: Hydrological Model Assessment and Development. R package version 0.9-26.

Beretta, C., et al. 2014. “Moisture Content Behaviour in Extensive Green Roofs during Dry Periods: the Influence of Vegetation and Substrate Characteristics.” *J Hydrol*, http://dx.doi.org/10.1016/j.jhydrol.2014.01.036.

Brenneisen, S. 2006. “Space for Urban Wildlife: Designing Green Roofs as Habitats in Switzerland.” *Urban Habitats*, 4 (1), 1541–7115. Accessed March 17, 2020. https://www.urbanhabitats.org.

Campbell Scientific. 2006. “CS616 and CS625 water content reflectometers,” Edmonton, Alberta. Available at https://s.campbellsci.com/documents/us/manuals/cs616.pdf, viewed February 19, 2016.

Carson, T., et al. 2017. “Assessing methods for predicting green roof rainfall capture: A comparison between full-scale observations and four hydrologic models.” *Urban Water J*, 14, 589–603. https://doi:10.1080/1573062X.2015.1056742.

Carson, T. B., et al. 2013. “Hydrological performance of extensive green roofs in New York City: observations and multi-year modeling of three full-scale systems.” *Environ Res Lett*, 8, 1-13. https://doi:10.1088/1748-9326/8/2/024036.

Carter, T. L. and T. C. Rasmussen. 2006. “Hydrologic behavior of vegetated roofs.” *J Am Water Res Assoc*, 42 (5), 1261-1274.

Castleton, H. F., et al. 2010. “Green roofs: Building energy savings and the potential for retrofit.” *Energ Buildings*, 42 (10), 1582-1591. https://doi:10.1016/j.enbuild.2010.05.004.

Chin, D. A. 2019. “Estimating Peak Runoff Rates Using the Rational Method.” *J Irrig Drain E*, 145, 04019006. https://doi:10.1061/(ASCE)IR.1943-4774.0001387.

Culligan, P. J., et al. 2014. Evaluation of Green Roof Water Quantity and Quality Performance in an Urban Climate. *US EPA report,* 1-79.

DiGiovanni, K., et al. 2013. “Applicability of Classical Predictive Equations for the Estimation of Evapotranspiration from Urban Green Space: Green Roof Results.” *J Hydrol Eng*, 18, 99-107.

Dingman, S.L. Stream Response to Water Input Events. In *Physical Hydrology*, 2nd ed.; Prentice Hall: New Jersey, USA, 2002; pp. 389-456.

Dooge, J. C. I. 1957. "The Rational method for estimating flood peaks." *Engineering*. 184, 311–313, 374–377.

D'Orazio, M., et al. 2012. "Green roof yearly performance: A case study in a highly insulated building under temperate climate," *Energ Buildings*, 55, 439-51.

Dunnett, N. and N. Kingsbury, 2004. *Planting Green Roofs and Living Walls*, TimberPress, Portland, OR.

Elliott, R.M., et al. 2016. "Green roof seasonal variation: Comparison of the hydrologic behavior of a thick and a thin extensive system in New York City." *Environ Res Lett*, 11, 074020.

Eumorfopoulou, E. and D. Aravantinos. 1998, "The contribution of a planted roof to the thermal protection of buildings in Greece." *Energ Buildings*, 27, 29-36.

Fassman-Beck, E. and D. Roehr. 2015. *Living Roofs in Integrated Urban Water Systems*. Routledge, New York.

Fassman-Beck, E., et al. 2016. "Curve Number and Runoff Coefficients for Extensive Living Roofs." *J Hydrol Eng*, 21 (3): 04015073. https://doi:10.1061/(ASCE)HE.1943-5584.0001318.

Fassman-Beck, E., et al. 2013. "4 Living roofs in 3 locations: Does configuration affect runoff mitigation." *J Hydrol*, 490, 11-20.

Feng, C., et al. 2010. "Theoretical and experimental analysis of the energy balance of extensive green roofs." *Energ Buildings*, 42 (6), 959-965. https://doi:10.1016/j.enbuild.2009.12.014.

Fioretti, R., et al. 2010. "Green roof energy and water related performance in the Mediterranean climate." *Build. Environ*, 45, 1890-1904.

Gaffin, S., et al. 2005. "Energy balance modeling applied to comparison of green and white roof cooling efficiency." *Proceeding of the 3rd Annual Greening Rooftops for Sustainable Communities,* Washington, D.C., 1-11.

Gaffin, S., et al. 2010. "A temperature and seasonal energy analysis of green, white, and black roofs." Available at www.coned.com/newsroom/pdf/Columbia%20study%20on%20Con%20Edisons%20roofs.pdf, viewed February 26, 2016.

Getter, K.L., et al. 2011. "Seasonal heat flux properties of an extensive green roof in a Midwestern U.S. climate." *Energ Buildings*, 43 (12), 3548-57.

Getter, K. L., et al. 2009. “Carbon sequestration potential of extensive green roofs.” *Environ Sci Technol*, 43, 7564–7570, https://doi:10.1021/es901539x.

GRHC (Green Roofs for Healthy Cities). 2019. “Green roof and wall policy in North America: Regulations, Incentives, and Best Practices.” https://greenroofs.org/policy-resources

Gong, Y., et al. 2018. “Factors affecting runoff retention performance of extensive green roofs.” *Water*, *10*, 1-15.

Hakimdavar, R., et al. 2014. “Scale dynamics of extensive green roofs: Quantifying the effect of drainage area and rainfall characteristics on observed and modeled green roof hydrologic performance.” *Ecol Eng*, 73*,* 494-508.

Hathaway, A.M. et al. 2008. “A field study of green roof hydrologic and water quality performance.” *Trans ASABE*, 1, 37-44.

Hawkins, R. H., et al. 2009. *Curve Number Hydrology: State of the Practice*. American Society of Civil Engineers. ISBN 978-0-7844-7257-6.

Hawkins, R. H., et al. 2019. “Understanding the Basis of the Curve Number Method for Watershed Models and TMDLs.” *J Hydrol Engr*, 24 (7), 06019003. https://doi:10.1061/(ASCE)HE.1943-5584.0001755.

Hill, J., et al. 2017. “Influences of Four Extensive Green Roof Design Variables on Stormwater Hydrology.” *J Hydrol Eng*, 22 (8), p04017019. https://doi:10.1061/(ASCE)HE.1943-5584.0001534.

Jiang, R. 2001. “Investigation of runoff curve number initial abstraction ratio.” M.S. thesis, Dept. of School of Natural Resources Watershed Management, Univ. of Arizona.

Jim, C.Y. and S.W. Tsang. 2011. “Ecological energetics of tropical intensive green roof,” *Energ Buildings,* 43 (10), 2696-704.

Johannessen, B. G., et al. 2018. “Detention and retention behavior of four extensive green roofs in three Nordic climate zones.” *Water-SUI,* 10, 1–23. https://doi:10.3390/w10060671.

Kottek, M., et al. 2006. “World map of the Köppen-Geiger climate classification updated.” *Meteorol Z,* 15, 259-263.

Kuichling, E. 1889. “The Relation Between the Rainfall and the Discharge of Sewers in Populous Districts.” *T Am Soc Civ Eng*, XX, 1–56.

Kumar, R. and S. C. Kaushik. 2005. “Performance evaluation of green roof and shading for thermal protection of buildings.” *Build Environ*, 40, 1505-1511. https://doi:10.1016/j.buildenv.2004.11.015.

Kurtz, T. 2008. “Flow monitoring of three ecoroofs in Portland, Oregon.” In proceedings: *Low Impact Development for Urban Ecosystem and Habitat Protection,* Seattle, Washington, USA November 16-19, 1-10.

Lazzarin, R. M., et al. 2005. “Experimental measurements and numerical modelling of a green roof.” *Energ Buildings*, 37, 1260-1267. https://doi:10.1016/j.enbuild.2005.02.001.

Li, Y. and R. W. Babcock. 2014. “Green roof hydrologic performance and modeling: A review.” *Water Sci Technol*, 69.4, 727-738. https://doi:10.2166/wst.2013.770.

Liu, K. and J. Minor. 2005. “Performance evaluation of an extensive green roof.” *Proceedings of the 3rd Annual Greening Rooftops for Sustainable Communities*, Washington, D.C., 1-11.

Liu, K. and B. Baskaran. 2003. “Thermal performance of green roofs through field evaluation.” *Proceedings of the First North American Green Roof Infrastructure Conference, Awards, and Trade Show*, Chicago, IL, 1-10.

Liu, X. and T.F.M. Chui. 2019. “Evaluation of green roof performance in mitigating the impact of extreme storms.” *Water*, 11*,* 1-13.

Loiola, C., et al. 2019. “Hydrological performance of modular-tray green roof systems for increasing the resilience of mega-cities to climate change.” *J Hydrol*, 573, 1057-1066. https://doi.org/10.1016/j.jhydrol.2018.01.004.

Lundholm, J.T., et al. 2014. “Snow depth and vegetation type affect green roof thermal performance in winter.” *Energ Buildings*, 84, 299-307.

Marasco, D.E.; et al. 2014. “Quantifying evapotranspiration from urban green roofs: A comparison of chamber measurements with commonly used predictive methods.” *Environ Sci Technol*, 48, 10273-10281.

McCuen, R. 2005. “Rational Method.” Hydrologic Analysis and Design. 3rd ed. 377-385. Upper Saddle River, New Jersey: Pearson Prentice Hall.

McGill, R., et al. 1978. “Variations of box plots.” *The American Statistician*, 32, 12-16.

Mentens, J., et al. 2006. “Green roofs as a tool for solving the rainwater runoff problem in the urbanized 21st century?” *Landsc and Urban Plan,* 77, 217-226.

Monge, Z. 2021 Personal Correspondence. Jacobs Engineering.

Mulvaney, T. 1851. “On the use of self-registering rain and flood gauges in making observations of the relations of rainfall and flood discharges in a given catchment.” *Proc Inst Civ Eng Ireland*. 42, 18–31.

NCEI (National Centers for Environmental Information) “Climate data online,” Available at

www.ncdc.noaa.gov, viewed August 6, 2016.

National Operational Hydrologic Remote Sensing Center "Snow depth observations for NY-OG-2 - DE WITT 1.4 WSW, NY," Available at www.nohrsc.noaa.gov, viewed February 26, 2016.

Nawaz, R., et al. 2015. "Hydrological performance of a full-scale extensive green roof located in a temperate climate." *Ecol Eng,* 82, 66-80.

Nelson, A. C. 2004. *Toward a New Metropolis: The Opportunity to Rebuild America.* The Brookings Institution, Washington D.C.

Niachou, A., et al. 2001. "Analysis of the green roof thermal properties and investigation of its energy performance." *Energ Buildings*, 33 (7), 719-29.

NRC-NRCC (Northeast Regional Climate and Natural Resources Conservation Center). Extreme Precipitation in New York & New England: An Interactive Web Tool for Extreme Precipitation Analysis. Available online: precip.eas.cornell.edu (accessed August 6, 2016).

NYC (New York City) Administrative Code § 28-601.1, 11 (2021). Accessed April 19, 2021. https://codelibrary.amlegal.com/codes/newyorkcity/latest/NYCadmin/0-0-0-69094.

NYC Environmental Protection. 2018. *New York City Stormwater Design Manual.* 1-169.

NYSDEC (New York State Department of Environmental Conversation). 2015. *Stormwater Management Design Manual*. Albany, NY.

Oliveira, P. T. S., et al. 2016. "Curve number estimation from Brazilian Cerrado rainfall and runoff data." *J Soil Water Conserv*, 71, 420–429. https://doi:10.2489/jswc.71.5.420.

Pearlmutter, D. and S. Rosenfeld. 2008. "Performance analysis of a simple roof cooling system with irrigated soil and two shading alternatives." *Energ Buildings*, 40 (5), 855-64.

Penn State University Agricultural Analytical Services Laboratory, test package GR01A.

Philadelphia Water Department. 2020. *Stormwater Management Guidance Manual.* v 3.2. 1-763.

Razzaghmanesh, M. and S. Beecham. 2014. "The hydrological behavior of extensive and intensive green roofs in a dry climate." *Sci Total Environ,* 499, 284-296.

Renewable Resource Data Center. "National solar radiation data base." Available at rredc.nrel.gov/solar/old_data/nsrdb (viewed March 14, 2016)

Roofscapes. 2011. "OnCenter green roof final technical specifications for bid." Available at savetherain.us/str_project/oncenter-green-roof/ (viewed June 2, 2016)

Rowe, D.B. 2011. “Green roofs as a means of pollution abatement.” Environ Pollut. 159, 2100-2110. https://doi:10.1016/j.envpol.2010.10.029

Sailor, D.J., et al. 2012. “Exploring the building energy impacts of green roof design decisions - a modeling study of buildings in four distinct climates.” J Building Physics, 35 (4), 372-91.

Schärer, L. A., et al. “Limitations in using runoff coefficients for green and gray roof design.” *Hydrol Res*, 51, 339–350. https://doi:10.2166/nh.2020.049.

Schroll, E., et al. 2011. “The role of vegetation in regulating stormwater runoff from green roofs in a winter rainfall climate.” *Ecol Eng,* 37, 595-600.

Sims, A. W., et al. 2019. “Mechanism controlling green roof peak flow rate attenuation.” *J Hydrol*, 577, 1-13.

Spolek, G. 2008. “Performance monitoring of three ecoroofs in Portland, Oregon.” *Urban Ecosyst,* 11, 349-359.

Speak, A. F., et al. 2013. “Rainwater runoff retention on an aged intensive green roof.” *Sci Total Environ,* 461-462, 28-38.

Squier, M. and C. I. Davidson. 2016. “Heat flux and seasonal thermal performance of an extensive green roof.” *Build Environ*, 107, 235-244. https://doi:10.1016/j.buildenv.2016.07.025.

Squier-Babcock, M. and C. I. Davidson. 2020. “Hydrologic performance of an extensive green roof system in Syracuse, NY.” *Water-SUI*, 12, 1–18. https://doi:10.3390/w12061535.

Starry, O., et al. 2014. “Photosynthesis and water use by two Sedum species in green roof substrate.” *Environ Exp Bot,* 107, 105-112.

Stovin, V. 2010. “The potential of green roofs to manage Urban Stormwater.” *Water Environ J,* 24, 192-199.

Stovin, V., et al. 2012. “The hydrologic performance of a green roof test bed under UK climatic conditions.” *J Hydrol,* 414-415, 148-161.

Stovin, V. et al. 2017. “Defining green roof detention performance.” *Urban Water J,* 14, 574-588.

Takebayashi, H. and M. Moriyama. 2007. “Surface heat budget on green roof and high reflection roof for mitigation of urban heat island.” *Build Environ,* 42 (8), 2971-79.

Theodosiou, T., et al. 2014. “Thermal behaviour of a green vs. a conventional roof under Mediterranean climate conditions.” *Int J Sust Energ*, 33 (1), 227-41.

Theodosiou, T.G. 2003. “Summer period analysis of the performance of a planted roof as a

passive cooling technique." *Energ Buildings*, 35 (9), 909-17.

Tsang, S.W. and C.Y. Jim. 2011. "Theoretical evaluation of thermal and energy performance of tropical green roofs." *Energy*, 36 (5), 3590-98.

Tukey, J.W. Exploratory Data Analysis; Addison-Wesley, 1977.

USDA. 1972. Part 630 Hydrology National Engineering Handbook Chapter 10 Estimation of Direct Runoff from Storm Rainfall. *National Engineering Handbook*.

USDA. 1986. Urban Hydrology for Small Watersheds. *Soil Conservation Service.*

van Renterghem, T. and D. Botteldooren. 2009. "Reducing the acoustical facade load from road traffic with green roofs." *Build Environ*, 44, 1081-1087. https://doi:10.1016/j.buildenv.2008.07.013.

van Renterghem, T. and D. Botteldooren. 2011. "In-situ measurements of sound propagating over extensive green roofs." *Build Environ*, 46, 729-738. https://doi:10.1016/j.buildenv.2010.10.006.

Van Spengen, J. 2010. The effects of large-scale green roof implementation on the rainfall-runoff in a tropical urbanized catchment. M.S. Thesis, Delft University of Technology, Netherlands.

Vesuviano, G., et al. 2013. "A two-stage storage routing model for green roof runoff detention." *Water Sci Technol*, 69(6), 1-7. https://doi:10.2166/wst.2013.808.

Voyde, E., et al. 2010. "Hydrology of an extensive living roof under sub-tropical climatic conditions in Auckland, New Zealand. *J Hydrol*. 394, 384-395.

Voyde, E., et al. 2010. "Quantifying evapotranspiration rates for New Zealand Green Roofs." *J Hydrol Eng,* 15, 395-403.

Wickham, H. *ggplot2: Elegant Graphics for Data Analysis*; Springer-Verlag: New York, 2016; https://ggplot2.tidyverse.org.

Wong, G.K.L. and C.Y. Jim. 2014. "Quantitative hydrologic performance of extensive green roof under humid tropical rainfall regime." *Ecol Eng*, *70*, 366-378.

Wong, N.H., et al. 2003a. "Investigation of thermal benefits of rooftop garden in the tropical environment." *Build Environ*, 38, 261-70.

Wong, N.H., et al. 2003b. "The effects of rooftop garden on energy consumption of a commercial building in Singapore." *Energ Buildings*, 35, 353-64.

Yang, Y. and C.I. Davidson. “Green roof performance influenced by growth medium characteristics.” Poster presented at: 15th Annual New York State Green Building Conference, USA, 2017 March 30-31.

Yang, Y. 2020. Evaluating the Hydrologic and Thermal Peformance of a Green Roof in Syracuse: Measurements and Modeling of a Full-Scale System. Ph.D. Dissertation. Syracuse University, Syracuse, NY.

Yang, Y. and C. I. Davidson, 2021. “Green roof aging effect on physical properties and hydrologic performance”, *J. Sustain. Water Built Environ.*, 7, 3, p04021007 (10pp.) https://ascelibrary.org/doi/abs/10.1061/JSWBAY.0000949?af=R.

Zhao, M., et al. 2014. “Effects of plant and substrate selection on thermal performance of green roofs during the summer.” *Build Environ,* 78, 199-211.

Zhao, M., et al. 2015. “Accumulated snow layer influence on the heat transfer process through green roof assemblies.” *Build Environ,* 87, 82-91.

Zhao, M., et al. 2013. “Comparison of green roof plants and substrates based on simulated green roof thermal performance with measured material properties.” *Proceedings of the 13th Conference of International Building Performance Simulation Association*, Chambéry, France, 817-23.

Zinzi, M. and G. Fasano. 2009. “Properties and performance of advanced reflective paints to reduce the cooling loads in buildings and mitigate the heat island effect in urban areas.” *Int J Sust Energ,* 28 (1-3), 123-39.

VITA

Mallory Squier-Babcock

Education

Syracuse University, ***PhD Candidate****, Civil and Environmental Engineering* ..... June 2023
Certificate of Advanced Study in Sustainable Enterprise (CASSE) ..... May 2013
Carnegie Mellon University, ***M.S.****, Civil and Environmental Engineering* ..... May 2010
Pennsylvania State University, ***B.S.****, Environmental Systems Engineering*..... May 2009
B.S., *Applied Spanish* ..... May 2009

Journal Publications

Squier-Babcock, M. and C.I. Davidson. 2023. "Green roofs in our cities: An analysis of two commonly-used modeling methods for the application of green roof technology." *J. Sustain. Water Built Environ.*, In Review.

Squier-Babcock, M. and C.I. Davidson. 2020. "Hydrologic performance of an extensive green roof system in Syracuse, NY." *Water-SUI*, 12, 1–18. https://doi:10.3390/w12061535.

Squier, M. and C.I. Davidson. 2016. "Heat flux and seasonal thermal performance of an extensive green roof." *Build Environ*, 107, 235-244. https://doi:10.1016/j.buildenv.2016.07.025.

Conference Proceedings

Davidson, C.I., C.D. Flynn, C. Gunawardana, A.J. Johnson, **M.N. Squier**, L.L. Worthen, and Y. Yang. 2018."The Use of a Large, Extensive Green Roof for Multiple Research Objectives" *International Building Physics Conference 2018*. 4.

Acharya, S., K. Ghadge, P. Uchil, C.D. Flynn, A.J. Johnson, **M.N. Squier,** Y. Yang, X. Yang, C.I. Davidson, G. Ameta, S. Rachuri, and A. Chakrabarti. 2017. Supporting Sustainable Service-System Design: A Case Study on Green-Roof Design with InDeaTe Template and Tool at Syracuse, New York. In: Chakrabarti, A., Chakrabarti, D. (eds) Research into Design for Communities, Volume 2. ICoRD 2017. Smart Innovation, Systems and Technologies, vol 66. Springer, Singapore. https://doi.org/10.1007/978-981-10-3521-0_2

Flynn, C.D., **M. Squier**, and C.I. Davidson. 2016. "Development of a case-based teaching module to improved student understanding of stakeholder engagement processes within engineering systems design." In Leal Filho, W., Nesbit, S. (eds) New Developments in Engineering Education for Sustainable Development. Word Sustainability Series, Springer, Cham. https://doi.org/10.1007/978-3-319-32933-8_6

Squier, M. N., J.B. Ahmad, Z. Cui, & C.I. Davidson. 2014. "Preliminary heat transfer analysis for a large extensive green roof." In *ICSI 2014: Creating Infrastructure for a Sustainable World* (pp. 1077-1085).

Select Conference Presentations

Squier, M. and Davidson, C. (2016) "Hydrologic performance of a large extensive green roof and the physical processes that govern performance," *presented at the* International Low Impact Development Conference, ASCE-EWRI, Portland, ME.

Squier, M. and Davidson, C. (2015). "Hydrologic Monitoring and Performance: The OnCenter Green Roof," *presented at the* International Low Impact Development Conference, ASCE-EWRI, Houston, TX.

Professional Experience

Civil Engineer, LaBella Associates DPC, Buffalo, NY February 2021 – *present*

- Oversaw the preparation of SWPPP documents for 50+ public and private clients under varying jurisdictions (MS4s and NY State).
- Prepare site design project documents from concept to construction documents for public and private clients.

Project Engineer, EDR, DPC, Syracuse, NY May 2017 – January 2021

- Oversaw the preparation of ESC plan and SWPPP documents for 40+ public and private clients under varying jurisdictions (City of Syracuse, MS4s, and NY State).
- Prepare site design project documents from concept to construction documents for public and private clients on 30+ projects including stadiums, university buildings, solar facilities, utility infrastructure improvements, and high-end residences.
- Author code to model ice throw from wind turbines and develop the report template as a new service offering - $32,000+. Submitted the first approved ice throw model to the Ohio Power Siting Board.
- Supervised project work for 11 entry level employees over 3.5 years.
-

Teaching Assistant, Syracuse University, Syracuse, NY August 2010 – May 2017

CIE 274: *Sustainability in Civil and Environmental Systems* (6 semesters)

- Taught once-weekly recitation for 30 students
- Developed course materials, including quiz and homework problems
- Held one-on-one meetings with struggling students
- Developed stakeholder engagement unit and co-taught to entire course (70-110 students)

ECS/CIE 400/600: *Introduction to Sustainable Engineering* (1 semester)

- Assisted in graduate level course of 23 students
- Developed curriculum and taught two-lecture mini-course on Life Cycle Analysis (LCA)

Corporate Env. Affairs Intern, PPG Industries, Pittsburgh, PA May 2008 – August 2008

- Managed global greenhouse gas emissions and environmental indicator metrics database
- Researched and advised on new greenhouse gas database management systems
- Prepared site history summaries for newly acquired facilities in Europe

Energy Technology Intern, Chevron, Houston, TX May 2007 – August 2007

- Developed spreadsheet to compile global use data for waste disposal facilities and analyzed for overlap
- Examined air quality issues related to flaring and venting and prepared technical summary of air quality
- Developed a spreadsheet to compile and analyze air emissions data gathered from well fields

Certificates and Awards

2nd Place PhD Category Student Poster Competition, Syracuse Center of Excellence, Syracuse, NY 2015
Outstanding Teaching Assistant Award, Syracuse University, Syracuse NY 2013-2014
Awarded to the top 4% of teaching assistants university-wide
US DOT TranLIVE Graduate Student of the Year, Syracuse University, Syracuse, NY 2013-2014
Recipient, Sustainable Enterprise Partnership Mini-Grant ($7000) 2012
Recipient, Carnegie Mellon Graduate Research Assistantship ($12000) 2009
Awarded to less than 10% of incoming students

Professional Service, Affiliations, and Activities

2023 – *present* **Member,** *American Society of Civil Engineers (ASCE)*
2012 – 2017 **Graduate Student Hearings Panelist,** *Academic Integrity Office, Syracuse University*
2013 – 2017 **Student Member,** *American Society of Civil Engineers (ASCE)-Environmental & Water Resources Institute (EWRI)*
2015 – 2016 **Secretary and Founding Member,** *ASEE at SU, Syracuse University*

2013 – 2015 **VP of Events and Founding Member, Net Impact,** *Syracuse Chapter, Syracuse University*
2013 – 2014 **Graduate Student Representative,** *Academic Affairs Committee, Syracuse University*
2012, 2014 **Curriculum Consultant,** *Project ENGAGE, Syracuse University*

License and Training

Professional Engineer – Approved to sit exam, *scheduled July 2023*
Engineer-In-Training (EIT) PA, May 2009
Current NYS DEC 4-hour Erosion & Sediment Control Training

Software

AutoCAD Civil 3D, HydroCAD, Autodesk Hydrographs Hydraflow, R, Microsoft Office, ForgeSolar, Revu BlueBeam, ProCore, Newforma, ArcGIS